AIMS Mathematics

http://www.aimspress.com/journal/Math

AIMS Mathematics, 11(8): 24241–24281
DOI: 10.3934/math.2026979
Received: 28 May 2026
Revised: 08 July 2026
Accepted: 29 July 2026
Published: 10 August 2026

Research article

Advancing reliability analysis for inverted Nadarajah–Haghighi distribution under adaptive progressive censoring with binomial removals

Refah Alotaibi[1], **Mazen Nassar**[2,3,*] **and Ahmed Elshahhat**[4]

[1] Department of Mathematical Sciences, College of Science, Princess Nourah bint Abdulrahman University, P.O. Box 84428, Riyadh 11671, Saudi Arabia

[2] Department of Statistics, Faculty of Science, King Abdulaziz University, Jeddah 21589, Saudi Arabia

[3] Department of Statistics, Faculty of Commerce, Zagazig University, Zagazig 44519, Egypt

[4] Faculty of Technology and Development, Zagazig University, Zagazig 44519, Egypt

* **Correspondence:** Email: mmohamad3@kau.edu.sa; mezo10011@gmail.com.

Abstract: This work introduced a flexible and practically motivated inferential framework for modeling lifetime data under complex and asymmetric settings. In particular, we considered the inverted Nadarajah–Haghighi distribution, a flexible skewed model capable of capturing diverse lifetime behaviors, within an adaptive progressive Type-II censoring scheme with random binomial removals. This formulation reflects realistic experimental conditions where the number of removed units varies randomly across stages, providing a more accurate representation of practical reliability and survival studies. Within this framework, statistical inference was developed for the model parameters, the binomial removal parameter, and key reliability measures using both classical and Bayesian approaches. Maximum likelihood estimation was obtained via numerical optimization, and approximate confidence intervals were constructed based on the observed Fisher information matrix. From a Bayesian perspective, independent gamma priors were assumed for the model parameters, while a beta prior was specified for the binomial removal parameter. Posterior inference was carried out using Markov chain Monte Carlo methods to obtain point estimates and corresponding credible intervals. A comprehensive simulation study was conducted to assess the performance of the proposed estimators under various configurations of sample size and model parameters. Finally, the applicability and effectiveness of the proposed methodology were demonstrated through the analysis of two real datasets arising from environmental toxicology and economic geology.

Keywords: inverted Nadarajah–Haghighi distribution; reliability measures; adaptive progressive censoring; binomial removal; loss function
Mathematics Subject Classification: 62F10, 62F15, 62N01, 62N05

1. Introduction

In recent decades, rapid technological advancements have significantly increased the lifetime and reliability of modern products. As a result, traditional life-testing procedures, such as complete sampling or classical single-stage censoring schemes including Type-I and Type-II censoring, have become less practical in many applications. These conventional approaches often require long observation periods to record a sufficient number of failures, which leads to increased cost and time. To address these limitations, more flexible and efficient censoring mechanisms, particularly multi-stage censoring schemes, have been developed and widely adopted in reliability and survival analysis. Among the existing approaches, the progressive Type-II censoring (PTIIC) scheme has received considerable attention due to its flexibility in removing surviving units during the experiment. This scheme allows the experimenter to withdraw a predetermined number of surviving items at each observed failure time, thereby reducing the overall test duration while maintaining adequate statistical information. Detailed discussions on progressive censoring schemes can be found in Balakrishnan [1]. One may also refer to the work of Brito et al. [2], Khalifa et al. [3], and Hasaballah et al. [4], among others.

To further improve the efficiency of progressive censoring, Ng et al. [5] introduced the adaptive PTIIC (APTIIC) scheme as an extension of the progressive Type-I hybrid censoring plan proposed by Kundu and Joarder [6]. In the progressive Type-I hybrid censoring scheme, the experiment terminates at a random time defined as the minimum of a pre-specified time T and the occurrence of a predetermined number of failures. Although this design provides control over the test duration, it may result in an insufficient number of observed failures, which negatively affects the accuracy of statistical inference. The APTIIC scheme addresses this limitation through an adaptive mechanism. For more details, see Nassar and Abo-Kasem [7], and Panahi and Moradi [8]. Specifically, the experiment follows the PTIIC structure before reaching the preassigned time T. However, once the time T is exceeded, no further removals of surviving units are allowed. This adjustment ensures that a sufficient number of failures is observed while maintaining flexibility in the termination of the experiment. Consequently, the APTIIC scheme provides a more reliable and practically applicable framework compared to standard censoring plans. The APTIIC scheme has been widely adopted in the statistical literature for addressing inference problems in lifetime models arising in reliability and survival analysis. Notable contributions include those of Elshahhat and Nassar [9], Dutta et al. [10], Alrumayh et al. [11], and Kumari et al. [12].

The APTIIC scheme can be described as follows. Suppose that n identical units are placed under a life-testing experiment at time zero. Let m denote the predetermined number of failures, and let $(S_1, S_2, \ldots, S_m)$ represent the progressive censoring plan. In addition, a fixed termination time T is specified prior to the experiment. At the time of the i-th failure, denoted by $X_{i:m:n}$ for $i = 1, \ldots, m$, a number S_i of the remaining surviving units is randomly removed from the test. This process continues according to the predefined removal pattern. If the m-th failure occurs before time T, that is, if $X_{m:m:n} < T$, the experiment proceeds as a standard progressive Type-II censoring scheme and terminates at $X_{m:m:n}$. However, if the time T lies between two consecutive failure times, say, $X_{k:m:n} < T < X_{k+1:m:n}$ with $k + 1 < m$, then the censoring mechanism is modified. In this case, all removals are stopped after the d-th failure by setting $S_{k+1} = \cdots = S_{m-1} = 0$. The experiment continues until the m-th failure is observed, at which point all remaining surviving units are removed. The number of units removed at the final stage is given by $S_m = n - m - \sum_{i=1}^{k} S_i$.

Let $x_{1:m:n} < \cdots < x_{k:m:n} < T < x_{d+1:m:n} < \cdots < x_{m:m:n}$ denote an observed sample obtained under the APTIIC scheme from a continuous distribution with probability density function $f(x; \boldsymbol{\theta})$ and cumulative distribution function $F(x;\boldsymbol{\theta})$, where $\boldsymbol{\theta}$ is the unknown parameter vector. The corresponding removal pattern is given by $(S_1,\dots,S_k,0,\dots,0,S_m)$. The likelihood function based on this observed sample can be written as

$$L_1(\boldsymbol{\theta}|\underline{\mathrm{x}}) = C_1 \prod_{i=1}^{m} f(x_i;\boldsymbol{\theta}) \prod_{i=1}^{k} [1 - F(x_i;\boldsymbol{\theta})]^{S_i} [1 - F(x_m;\boldsymbol{\theta})]^{S_m}, \tag{1.1}$$

where C_1 is a normalizing constant and $\underline{\mathrm{x}} = (x_1,\dots,x_m)$ with $x_i = x_{i:m:n}$ for $i = 1,\dots,m$.

Selecting an appropriate statistical distribution to represent a population of interest is a fundamental step in modeling, as it directly influences the accuracy of reliability analysis and inference. In particular, the choice of a suitable lifetime model is crucial for capturing the underlying failure mechanism and for obtaining reliable estimates of key reliability measures. To address the limitation of the constant hazard rate property of the exponential distribution, Nadarajah and Haghighi [13] introduced the Nadarajah–Haghighi (NH) distribution, which offers greater flexibility while retaining the exponential model as a special case. Due to its tractability and adaptability, the NH distribution has been widely used in reliability and survival analysis. Motivated by the flexibility of the NH model, Tahir et al. [14] proposed the inverted Nadarajah–Haghighi (INH) distribution as an inverted version of the NH distribution. The INH distribution is characterized by one scale parameter and one shape parameter, and is capable of modeling lifetime data with decreasing as well as unimodal hazard rate functions (HRFs).

A random variable X is said to follow the INH distribution with scale parameter $\mu > 0$ and shape parameter $\sigma > 0$ if its probability density and distribution functions are given, respectively, by

$$f(x;\boldsymbol{\theta}) = \mu\sigma x^{-2}\left(1+\frac{\mu}{x}\right)^{\sigma-1} \exp\left\{1-\left(1+\frac{\mu}{x}\right)^{\sigma}\right\}, \quad x > 0, \tag{1.2}$$

and

$$F(x;\boldsymbol{\theta}) = \exp\left\{1-\left(1+\frac{\mu}{x}\right)^{\sigma}\right\}, \tag{1.3}$$

where $\boldsymbol{\theta} = (\mu,\sigma)^{\top}$. In what follows, a random variable whose probability density function is given in (1.2) will be denoted by $X \sim \mathrm{INH}(\boldsymbol{\theta})$. In addition, the reliability function (RF) and HRF of the INH distribution are given, respectively, by

$$R(x;\boldsymbol{\theta}) = 1 - \exp\left\{1-\left(1+\frac{\mu}{x}\right)^{\sigma}\right\} \tag{1.4}$$

and

$$h(x;\boldsymbol{\theta}) = \mu\sigma x^{-2}\left(1+\frac{\mu}{x}\right)^{\sigma-1} \left\{\exp\left[\left(1+\frac{\mu}{x}\right)^{\sigma}-1\right]-1\right\}^{-1}. \tag{1.5}$$

Despite the flexibility of the INH distribution, relatively limited attention has been given to the estimation of the INH distribution. Elshahhat and Rastogi [15] investigated parameter estimation under the PTIIC scheme. Abo-Kasem et al. [16] studied survival estimation within the adaptive progressive Type-II censoring framework. Abushal and Al-Zaydi [17] developed inference procedures under Type-II generalized hybrid censoring with competing risks. Mohammed et al. [18] examined optimal progressive and Bayesian inference under unified progressive hybrid censoring, while Alqasem et al. [19] focused on reliability estimation based on joint progressive Type-II censoring schemes.

The APTIIC scheme assumes that the number of units removed at each stage is fixed in advance. In many practical reliability experiments, however, this assumption may be unrealistic, as the removal process is often influenced by random operational conditions, resource availability, and observed failure patterns. In life-testing studies involving engineering components and industrial systems, experiments are frequently terminated early due to time and cost constraints, and the number of surviving units withdrawn at different stages may vary in an unpredictable manner. To account for such practical considerations, Elshahhat and Nassar [20] extended the APTIIC scheme by incorporating random removals, where the number of units removed at each stage is modeled as a binomial random variable. This modification enhances the flexibility of the censoring mechanism and provides a more realistic representation of real-world testing environments. For further details on the use of random removals in modeling the behavior of removal patterns, see Yuen and Tse [21], Wu and Chang [22], Sharafi [23], and Almetwally [24]. The incorporation of random removals allows the censoring scheme to capture stochastic and data-driven decision processes commonly encountered in industrial reliability studies. A detailed description of this extended censoring mechanism is presented in the next section.

To the best of our knowledge, no study has addressed the estimation of the model parameters and associated reliability measures of the INH distribution under the APTIIC scheme, whether with fixed or random removals, despite its flexibility in modeling lifetime data. In many practical applications, lifetime data exhibit clear asymmetry due to heterogeneity in operating conditions and variability in failure mechanisms. Classical symmetric models may fail to capture such features, leading to inaccurate inference. This has motivated the use of flexible skewed distributions capable of representing a wide range of lifetime behaviors and hazard rate shapes, among which the INH distribution provides a suitable and effective framework.

Motivated by this gap, and by the practical importance of incorporating random removals into adaptive life-testing experiments, this paper develops a comprehensive inferential framework for the INH distribution under the APTIIC scheme with binomial removals. The methodological contribution extends beyond applying an existing lifetime model under an existing censoring design. Specifically, a joint likelihood is formulated by integrating the lifetime model with the stochastic removal mechanism, providing a unified framework for simultaneous inference on both the lifetime distribution and the random-removal process. This unified formulation facilitates the development of both classical and Bayesian inferential procedures for model parameters and associated reliability measures. The proposed methodology is further evaluated through extensive Monte Carlo simulations and illustrated using two real datasets.

The main methodological contributions of this study are summarized as follows:

- A unified inferential framework is developed for the INH distribution under the APTIIC scheme with stochastic binomial removals.
- A joint likelihood function is derived by combining the lifetime and stochastic removal processes, enabling simultaneous estimation of the model parameters and the binomial removal parameter.
- Classical inference is developed through maximum likelihood estimation together with approximate confidence intervals (ACIs) for the model parameters and the associated reliability measures.
- A Bayesian inferential framework based on Markov chain Monte Carlo (MCMC) sampling is developed to obtain Bayes estimates and Bayes credible intervals (BCIs) for all unknown quantities.
- The finite-sample performance and practical applicability of the proposed inferential procedures are comprehensively assessed through Monte Carlo simulations and two real-data applications.

The remainder of the paper is organized as follows. Section 2 describes the APTIIC scheme with binomial removals and develops the maximum likelihood estimators (MLEs) and ACIs for the model parameters, the binomial removal parameter, and the associated reliability measures. Section 3 is devoted to Bayesian estimation under the squared error loss function. Section 4 presents the simulation study and discusses the obtained results. In Section 5, the proposed methods are applied to two datasets. Finally, Section 6 concludes the paper.

2. Modeling under APTIIC with binomial removals and likelihood estimation

In this section, we begin by presenting the APTIIC scheme with binomial removals. Afterward, the MLEs and ACIs of μ, σ, binomial distribution parameter, RF, and HRF are investigated.

2.1. APTIIC plan with random binomial removals

Consider a life-testing experiment that starts with n identical units placed under observation. Failures are recorded sequentially, and at the time of the ith observed failure, a random number of the remaining surviving units is withdrawn from the test. The number of removed units at each stage is assumed to follow a binomial mechanism, where each active unit is independently removed with a fixed probability. The censoring scheme evolves adaptively over time. Prior to a predetermined time T, removals are carried out according to a progressive censoring rule. Once the time T is reached, the removal process is terminated, and all remaining units continue to be observed until the required number of failures is achieved. This adaptive structure allows the experiment to balance practical constraints, such as time and cost, with the need to collect sufficient failure information.

Following Elshahhat and Nassar [20], let S_i denote the number of units removed at the ith stage, and assume that S_i follows a binomial distribution with parameter ϕ. This implies that each unit still under test at that stage has the same probability p of being removed. Let $n_i^\circ = n - m - \sum_{j=1}^{i-1} S_j$ denote the number of units at risk just before the ith removal stage. Then, the conditional probability mass function of S_i is given by

$$P(S_i = s_i \mid S_{i-1} = s_{i-1}, \ldots, S_1 = s_1) = \binom{n_i^\circ}{s_i} \phi^{s_i} (1-\phi)^{n_i^\circ - s_i}, \tag{2.1}$$

where $0 \le s_i \le n_i^\circ$, for $i = 1, \ldots, k$.

Consequently, the joint likelihood function of $\mathbf{S} = (S_1, \ldots, S_k)$ can be expressed as

$$L_2(\mathbf{S} = \mathbf{s}; \phi) = \prod_{i=1}^{k} P(S_i = s_i \mid S_{i-1}, \ldots, S_1). \tag{2.2}$$

Substituting (2.1) into (2.2) yields

$$L_2(\mathbf{S} = \mathbf{s}; \phi) = C_2\, \phi^{\varpi_1} (1-\phi)^{\varpi_2}, \tag{2.3}$$

where $C_2 = \prod_{i=1}^{k} \binom{n_i^\circ}{s_i}$, $\varpi_1 = \sum_{i=1}^{k} s_i$, and $\varpi_2 = \sum_{i=1}^{k} (n_i^\circ - s_i)$.

Assuming independence between the observed failure lifetimes and the removal counts at each stage, the joint likelihood function for the unknown parameter vector $\boldsymbol{\theta}$ and the binomial parameter ϕ can be formulated as the product of the corresponding likelihood components. Specifically, by combining (1.1) and (2.3), we obtain

$$L(\boldsymbol{\theta}, \phi; \underline{\mathbf{x}}, \mathbf{s}) = L_1(\boldsymbol{\theta} \mid \underline{\mathbf{x}})\, L_2(\mathbf{S} = \mathbf{s}; \phi). \tag{2.4}$$

In the following subsections, MLEs and ACIs for the model parameters and the associated reliability measures are developed based on APTIIC data with binomial removals, providing a flexible and realistic framework for modeling the removal mechanism.

2.2. Likelihood-based point estimation

Consider an observed APTIIC sample $\underline{\mathbf{x}}$ obtained from the INH distribution with removal pattern $(S_1, \ldots, S_d, 0, \ldots, 0, S_m)$, where $(S_1, \ldots, S_d)$ are generated according to a binomial removal mechanism. Using the probability density function in (1.2), the distribution function in (1.3), and the likelihood formulation in (1.1), the likelihood function of the unknown parameter vector $\boldsymbol{\theta}$, up to a proportionality constant, can be written as

$$\begin{aligned} L_1(\boldsymbol{\theta}; \underline{\mathrm{x}}, \mathbf{s}) &= \mu^m \sigma^m \exp\left\{(\sigma - 1)\sum_{i=1}^{m} \log(1+\mu x_i) - \sum_{i=1}^{m}(1+\mu x_i)^{\sigma}\right. \\ &+ \left.\sum_{i=1}^{k} S_i \log\left[1 - e^{1-(1+\mu x_i)^{\sigma}}\right] + S_m \log\left[1 - e^{1-(1+\mu x_m)^{\sigma}}\right]\right\}, \end{aligned} \tag{2.5}$$

where $x_i = x_i^{-1}$ for simplicity. The natural logarithm of (2.5) is as follows:

$$\begin{aligned} \mathcal{L}_1(\boldsymbol{\phi}; \underline{\mathrm{x}}, \mathbf{s}) &= m\log(\mu) + m\log(\sigma) + (\sigma - 1)\sum_{i=1}^{m} \log(1+\mu x_i) - \sum_{i=1}^{m}(1+\mu x_i)^{\sigma} \\ &+ \sum_{i=1}^{k} S_i \log\left[1 - e^{1-(1+\mu x_i)^{\sigma}}\right] + S_m \log\left[1 - e^{1-(1+\mu x_m)^{\sigma}}\right]. \end{aligned} \tag{2.6}$$

By differentiating the log-likelihood function in (2.6) with respect to μ and σ, and setting the resulting expressions equal to zero, we obtain the following system of likelihood equations:

$$\frac{\partial \mathcal{L}_1(\boldsymbol{\theta}; \underline{\mathrm{x}}, \mathbf{s})}{\partial \mu} = \frac{m}{\mu} + (\sigma - 1)\sum_{i=1}^{m} \frac{x_i}{y_i} - \sigma \sum_{i=1}^{m} y_i^{\sigma-1} x_i + \sigma \sum_{i=1}^{k} \frac{S_i y_i^{\sigma-1} x_i}{e^{y_i^{\sigma}-1} - 1} + \frac{\sigma S_m y_m^{\sigma-1} x_m}{e^{y_m^{\sigma}-1} - 1} \tag{2.7}$$

and

$$\frac{\partial \mathcal{L}_1(\boldsymbol{\theta}; \underline{\mathrm{x}}, \mathbf{s})}{\partial \sigma} = \frac{m}{\sigma} + \sum_{i=1}^{m} \log(y_i) - \sum_{i=1}^{m} y_i^{\sigma} \log(y_i) + \sum_{i=1}^{k} \frac{S_i y_i^{\sigma} \log(y_i)}{e^{y_i^{\sigma}-1} - 1} + \frac{S_m y_m^{\sigma} \log(y_m)}{e^{y_m^{\sigma}-1} - 1}, \tag{2.8}$$

where $y_i = 1 + \mu x_i$.

It is clear that closed-form expressions for the MLEs are not available due to the complexity of the likelihood equations in (2.7) and (2.8). These nonlinear equations must therefore be solved numerically to obtain the MLEs of μ and σ. In this study, an iterative numerical procedure, such as the Newton–Raphson algorithm, can be employed to compute the estimates, denoted by $\hat{\mu}$ and $\hat{\sigma}$. A key advantage of the maximum likelihood approach is the invariance property, which states that the MLE of any function of the parameters can be obtained by substituting the MLEs into that function. Accordingly, the MLEs of the RF and HRF at a given time t are obtained by replacing μ and σ with $\hat{\mu}$ and $\hat{\sigma}$ in (1.4) and (1.5), respectively, as

$$\hat{R}(t) = 1 - \exp\left\{1 - \left(1 + \frac{\hat{\mu}}{t}\right)^{\hat{\sigma}}\right\}$$

and

$$\hat{h}(t) = \hat{\mu}\hat{\sigma}t^{-2}\left(1 + \frac{\hat{\mu}}{t}\right)^{\hat{\sigma}-1}\left\{\exp\left[\left(1 + \frac{\hat{\mu}}{t}\right)^{\hat{\sigma}} - 1\right] - 1\right\}^{-1}.$$

In a similar manner, the MLE of the binomial removal parameter ϕ can be derived from (2.3). Ignoring the constant term, the corresponding log-likelihood function is given by

$$\mathcal{L}_2(\mathbf{S} = \mathbf{s}; \phi) = \varpi_1 \log(\phi) + \varpi_2 \log(1 - \phi). \tag{2.9}$$

Differentiating (2.9) with respect to ϕ and equating the result to zero yields the MLE of ϕ, denoted by $\hat{\phi}$, as

$$\hat{\phi} = \frac{\varpi_1}{\varpi_1 + \varpi_2}. \tag{2.10}$$

2.3. Interval estimation for unknown parameters

To construct interval estimates for the model parameters as well as the binomial parameter, it is necessary to obtain the variances of their corresponding MLEs. Under standard regularity conditions, the asymptotic distribution of the MLEs can be used to derive the ACIs. The asymptotic variance–covariance matrix of the estimators is obtained from the inverse of the Fisher information matrix. However, due to the complexity of the likelihood equations and the second-order derivatives involved, deriving the exact Fisher information matrix in closed form is not tractable in this case. To address this issue, the variance–covariance matrix is approximated by inverting the observed Fisher information matrix evaluated at the MLEs, denoted by $\hat{\boldsymbol{\theta}} = (\hat{\mu}, \hat{\sigma})^\top$. This approach provides a practical and efficient way to obtain the required standard errors for constructing ACIs. The estimated variance-covariance matrix can be expressed as

$$\begin{aligned} \boldsymbol{I}^{-1}(\hat{\boldsymbol{\theta}}, \hat{p}) &= \begin{bmatrix} -\frac{\partial^2 \mathcal{L}_1(\boldsymbol{\theta};\underline{\mathrm{x}},\mathbf{s})}{\partial \mu^2} & -\frac{\partial \mathcal{L}_1(\boldsymbol{\theta};\underline{\mathrm{x}},\mathbf{s})}{\partial \mu \partial \theta} & 0 \\ & -\frac{\partial^2 \mathcal{L}_1(\boldsymbol{\theta};\underline{\mathrm{x}},\mathbf{s})}{\partial \theta^2} & 0 \\ & & -\frac{\partial^2 \mathcal{L}_2(\mathbf{S}=\mathbf{s};\phi)}{\partial p^2} \end{bmatrix}^{-1}_{(\boldsymbol{\theta},\phi)=(\hat{\boldsymbol{\theta}},\hat{\phi})} \\ &= \begin{bmatrix} \widehat{\mathrm{var}}(\hat{\mu}) & \widehat{\mathrm{cov}}(\hat{\mu}, \hat{\sigma}) & 0 \\ & \widehat{\mathrm{var}}(\hat{\sigma}) & 0 \\ & & \widehat{\mathrm{var}}(\hat{\phi}) \end{bmatrix}. \end{aligned} \tag{2.11}$$

The elements of the observed Fisher information matrix are obtained by taking the second-order partial derivatives of the log-likelihood function with respect to the unknown parameters. These derivatives are calculated directly from the corresponding score equations and are presented below for completeness.

$$\frac{\partial \mathcal{L}_1(\boldsymbol{\theta}; \underline{\mathrm{x}}, \mathbf{s})}{\partial \mu^2} = -\frac{m}{\mu^2} - (\sigma - 1) \sum_{i=1}^{m} \frac{x_i^2}{y_i^2} - \sigma(\sigma - 1) \sum_{i=1}^{m} x_i^2 y_i^{\sigma-2} + \sigma \sum_{i=1}^{k} S_i a_i + \sigma S_m a_m,$$

$$\frac{\partial \mathcal{L}_1(\boldsymbol{\theta}; \underline{\mathrm{x}}, \mathbf{s})}{\partial \sigma^2} = -\frac{m}{\sigma^2} - \sum_{i=1}^{m} y_i^{\sigma} \log^2(y_i) + \sum_{i=1}^{k} S_i b_i + S_m b_m,$$

$$\frac{\partial \mathcal{L}_1(\boldsymbol{\theta}; \underline{\mathrm{x}}, \mathbf{s})}{\partial \mu \partial \sigma} = \sum_{i=1}^{m} \frac{x_i}{y_i} - \sum_{i=1}^{m} y_i^{\sigma-1} x_i - \sigma \sum_{i=1}^{m} x_i y_i^{\sigma-1} \log(y_i) + \sum_{i=1}^{k} S_i c_i + S_m c_m,$$

and

$$\frac{\partial^2 \mathcal{L}_2(\mathbf{S}=\mathbf{s};\phi)}{\partial \phi^2} = -\frac{\varpi_1}{\phi^2} - \frac{\varpi_2}{(1-\phi)^2},$$

where

$$a_i = x_i^2 y_i^{\sigma-2} \frac{(\sigma-1)(e^{y_i^{\sigma}-1}-1) - \sigma y_i^{\sigma-1} e^{y_i^{\sigma}-1}}{(e^{y_i^{\sigma}-1}-1)^2},\ b_i = y_i^{\sigma} \log^2(y_i) \frac{e^{y_i^{\sigma}-1}(1-y_i^{\sigma})-1}{(e^{y_i^{\sigma}-1}-1)^2},$$

and

$$c_i = x_i \left[\frac{y_i^{\sigma-1}}{e^{y_i^{\sigma}-1}-1} + \sigma y_i^{\sigma-1} \log(y_i) \frac{e^{y_i^{\sigma}-1}(1-y_i^{\sigma})-1}{(e^{y_i^{\sigma}-1}-1)^2} \right], i = 1, \ldots, m.$$

Under some mild regularity conditions, the MLEs of the model parameters are asymptotically normally distributed. Specifically, we have $(\hat{\boldsymbol{\theta}}, \hat{\phi}) \xrightarrow{d} \mathcal{N}\left[(\boldsymbol{\theta}, \phi), \boldsymbol{I}^{-1}(\hat{\boldsymbol{\theta}}, \hat{\phi})\right]$. Based on this asymptotic normality, the ACIs for the model parameters and the binomial parameter can be constructed. For a given confidence level $100(1-\alpha)\%$, the ACIs for μ, σ, and ϕ are given by

$$\left\{\hat{\mu} - z_{\alpha/2}\sqrt{\widehat{\text{var}}(\hat{\mu})},\ \hat{\mu} + z_{\alpha/2}\sqrt{\widehat{\text{var}}(\hat{\mu})}\right\}, \quad \left\{\hat{\sigma} - z_{\alpha/2}\sqrt{\widehat{\text{var}}(\hat{\sigma})},\ \hat{\sigma} + z_{\alpha/2}\sqrt{\widehat{\text{var}}(\hat{\sigma})}\right\},$$

and

$$\left\{\hat{\phi} - z_{\alpha/2}\sqrt{\widehat{\text{var}}(\hat{\phi})},\ \hat{\phi} + z_{\alpha/2}\sqrt{\widehat{\text{var}}(\hat{\phi})}\right\},$$

where $z_{\alpha/2}$ denotes the upper $(\alpha/2)$ quantile of the standard normal distribution.

2.4. Interval estimation for reliability measures

In reliability analysis, interval estimation of the RF and HRF provides additional insight into the uncertainty associated with these measures. To construct such intervals, it is necessary to approximate the variances of their corresponding MLEs. In this study, the delta method is employed for this purpose. Since both the RF and HRF depend only on the model parameters μ and σ, and are independent of the binomial removal parameter ϕ, their variances can be approximated using the variance–covariance matrix of $(\hat{\mu}, \hat{\sigma})^{\top}$. Specifically, the approximate variance of the MLE of the RF at time t is given by

$$\begin{aligned}
\widehat{\text{var}}(\hat{R}) &\approx \begin{bmatrix} \frac{\partial R(t)}{\partial \mu} & \frac{\partial R(t)}{\partial \sigma} \end{bmatrix} \begin{bmatrix} \widehat{\text{var}}(\hat{\mu}) & \widehat{\text{cov}}(\hat{\mu},\hat{\sigma}) \\ \widehat{\text{cov}}(\hat{\mu},\hat{\sigma}) & \widehat{\text{var}}(\hat{\sigma}) \end{bmatrix} \begin{bmatrix} \frac{\partial R(t)}{\partial \mu} \\ \frac{\partial R(t)}{\partial \sigma} \end{bmatrix} \\
&\approx \left[\frac{\partial R(t)}{\partial \mu}\right]^2 \widehat{\text{var}}(\hat{\mu}) + \left[\frac{\partial R(t)}{\partial \sigma}\right]^2 \widehat{\text{var}}(\hat{\sigma}) + 2\left[\frac{\partial R(t)}{\partial \mu}\right]\left[\frac{\partial R(t)}{\partial \sigma}\right]\widehat{\text{cov}}(\hat{\mu},\hat{\sigma}),
\end{aligned}$$

and similarly, the approximate variance of the MLE of the HRF is

$$\begin{aligned}
\widehat{\text{var}}(\hat{h}) &\approx \begin{bmatrix} \frac{\partial h(t)}{\partial \mu} & \frac{\partial h(t)}{\partial \sigma} \end{bmatrix} \begin{bmatrix} \widehat{\text{var}}(\hat{\mu}) & \widehat{\text{cov}}(\hat{\mu},\hat{\sigma}) \\ \widehat{\text{cov}}(\hat{\mu},\hat{\sigma}) & \widehat{\text{var}}(\hat{\sigma}) \end{bmatrix} \begin{bmatrix} \frac{\partial h(t)}{\partial \mu} \\ \frac{\partial h(t)}{\partial \sigma} \end{bmatrix} \\
&\approx \left[\frac{\partial h(t)}{\partial \mu}\right]^2 \widehat{\text{var}}(\hat{\mu}) + \left[\frac{\partial h(t)}{\partial \sigma}\right]^2 \widehat{\text{var}}(\hat{\sigma}) + 2\left[\frac{\partial h(t)}{\partial \mu}\right]\left[\frac{\partial h(t)}{\partial \sigma}\right]\widehat{\text{cov}}(\hat{\mu},\hat{\sigma}),
\end{aligned}$$

where the partial derivatives are evaluated at the MLEs $\hat{\mu}$ and $\hat{\sigma}$, and are given by

$$\frac{\partial R(t)}{\partial \mu} = -\frac{\sigma\left(1+\frac{\mu}{t}\right)^{\sigma}}{t+\mu} \exp\left\{1 - \left(1+\frac{\mu}{t}\right)^{\sigma}\right\},$$

$$\frac{\partial R(t)}{\partial \sigma} = -\left(1+\frac{\mu}{t}\right)^{\sigma} \log\left(1+\frac{\mu}{t}\right) \exp\left\{1-\left(1+\frac{\mu}{t}\right)^{\sigma}\right\},$$

$$\frac{\partial h(t)}{\partial \mu} = h(t)\left[\frac{1}{\mu}+\frac{\sigma-1}{t+\mu}-\frac{\sigma\left(1+\frac{\mu}{t}\right)^{\sigma}}{t+\mu}\left(1+\frac{1}{\exp\left\{\left(1+\frac{\mu}{t}\right)^{\sigma}-1\right\}-1}\right)\right],$$

and

$$\frac{\partial h(t)}{\partial \sigma} = h(t)\left[\frac{1}{\sigma}+\log\left(1+\frac{\mu}{t}\right)\left(1-\left(1+\frac{\mu}{t}\right)^{\sigma}-\frac{\left(1+\frac{\mu}{t}\right)^{\sigma}}{\exp\left\{\left(1+\frac{\mu}{t}\right)^{\sigma}-1\right\}-1}\right)\right].$$

Employing that $\hat{R}(t)$ and $\hat{h}(t)$ are asymptotically normally distributed, the $100(1-\alpha)\%$ ACIs for $R(t)$ and $h(t)$ are given by

$$\left\{\hat{R}(t) - z_{\alpha/2}\sqrt{\widehat{\mathrm{var}}(\hat{R})},\ \hat{R}(t) + z_{\alpha/2}\sqrt{\widehat{\mathrm{var}}(\hat{R})}\right\}$$

and

$$\left\{\hat{h}(t) - z_{\alpha/2}\sqrt{\widehat{\mathrm{var}}(\hat{h})},\ \hat{h}(t) + z_{\alpha/2}\sqrt{\widehat{\mathrm{var}}(\hat{h})}\right\}.$$

3. Bayesian estimation

In this section, Bayesian inference is developed for the unknown parameters of the INH distribution, along with the associated RF and HRF, based on APTIIC data with binomial removals. Point estimates and BCIs are obtained within this framework. The analysis is conducted under the squared error loss function; however, other loss functions may also be considered.

3.1. Prior specification and posterior distributions

A key step in Bayesian analysis is the specification of suitable prior distributions for the unknown parameters. Inspection of the likelihood function in (2.5) shows that no conjugate prior distributions are available for the model parameters. Since the parameters μ and σ are defined on the positive real line $(0,\infty)$, it is natural to adopt gamma priors for both parameters due to their flexibility and compatibility with the parameter space. Accordingly, we assume that μ and σ are independent and follow gamma distributions, namely, $\mu \sim \text{Gamma}(\tau_1, \epsilon_1)$, and $\sigma \sim \text{Gamma}(\tau_2, \epsilon_2)$, where $\tau_j > 0$ and $\epsilon_j > 0$, $j = 1, 2$, are known hyperparameters. Under this assumption, the joint prior distribution of $\boldsymbol{\theta}$ can be expressed as

$$g_1(\boldsymbol{\theta}) \propto \mu^{\tau_1-1}\sigma^{\tau_2-1}\exp\left\{-(\epsilon_1\mu+\epsilon_2\sigma)\right\}, \quad \mu,\sigma>0. \tag{3.1}$$

For the binomial removal parameter ϕ, which lies in the interval $(0,1)$, the beta distribution provides a natural prior choice. Specifically, we assume $\phi \sim \text{Beta}(\tau_3, \epsilon_3)$, where $\tau_3 > 0$ and $\epsilon_3 > 0$ are hyperparameters. The corresponding prior density is given by

$$g_2(\phi) \propto \phi^{\tau_3-1}(1-\phi)^{\epsilon_3-1}, \quad 0<\phi<1. \tag{3.2}$$

Since the model parameters are independent of the binomial removal parameter, the posterior distributions can be derived separately to simplify the inference procedure. By combining the likelihood function in (2.5) with the joint prior distribution in (3.1), the posterior distribution of the parameter vector $\boldsymbol{\theta}$ can be expressed as follows:

$$\begin{aligned} G_1(\boldsymbol{\theta}|\underline{\mathrm{x}}, \mathbf{s}) &= \frac{1}{A}\mu^{m+\tau_1-1}\sigma^{m+\tau_2-1}\exp\left\{(\sigma-1)\sum_{i=1}^{m}\log(1+\mu x_i) - \sum_{i=1}^{m}(1+\mu x_i)^{\sigma}\right. \\ &+ \left.\sum_{i=1}^{k} S_i \log\left[1-e^{1-(1+\mu x_i)^{\sigma}}\right] + S_m \log\left[1-e^{1-(1+\mu x_m)^{\sigma}}\right] - \epsilon_1\mu - \epsilon_2\sigma\right\}, \end{aligned} \quad (3.3)$$

where the normalized constant A is defined as follows:

$$A = \int_0^{\infty}\int_0^{\infty} g_1(\boldsymbol{\theta})L_1(\boldsymbol{\theta}|\underline{\mathrm{x}}, \mathbf{s})d\mu d\sigma.$$

By combining the likelihood function in (2.3) with the prior distribution in (3.2), and simplifying the resulting expression, the posterior distribution of the binomial parameter ϕ is obtained as

$$G_2(\phi \mid \mathbf{s}) = \frac{\phi^{\varpi_1+\tau_3-1}(1-\phi)^{\varpi_2+\epsilon_3-1}}{B(\varpi_1+\tau_3,\ \varpi_2+\epsilon_3)}, \quad (3.4)$$

where $B(\cdot,\cdot)$ denotes the beta function.

3.2. Bayes estimation and credible intervals

Since the posterior distribution of the binomial parameter ϕ is available in closed form, as given in (3.4), its Bayesian inference can be carried out directly without the need for numerical approximation. Under the squared error loss function, the Bayes estimator of ϕ is given by the posterior mean. Accordingly, the Bayes estimate of ϕ is obtained as

$$\tilde{\phi} = \frac{\varpi_1+\tau_3}{\varpi_1+\varpi_2+\tau_3+\epsilon_3}.$$

To construct the BCI for ϕ, consider a credibility level of $100(1-\alpha)\%$. The interval bounds, denoted by ϕ_L and ϕ_U, are determined such that the posterior probability within this interval equals $1-\alpha$. That is,

$$\frac{1}{B(\varpi_1+\tau_3,\ \varpi_2+\epsilon_3)}\int_{\phi_L}^{\phi_U}\phi^{\varpi_1+\tau_3-1}(1-\phi)^{\varpi_2+\epsilon_3-1}\,d\phi = 1-\alpha. \quad (3.5)$$

The interval $[\phi_L, \phi_U]$ is constructed such that it contains the true value of the parameter ϕ with posterior probability $1-\alpha$. Based on (3.5), the endpoints of the BCI can be obtained from the quantiles of the corresponding beta distribution as

$$\{\mathscr{B}(\varpi_1+\tau_3,\ \varpi_2+\epsilon_3;\ \alpha/2)\,,\ \mathscr{B}(\varpi_1+\tau_3,\ \varpi_2+\epsilon_3;\ 1-\alpha/2)\}\,,$$

where $\mathscr{B}(\cdot,\cdot;\cdot)$ denotes the quantile function of the beta distribution.

For the model parameters, or for any function of them, say, $\psi(\boldsymbol{\theta})$, the Bayes estimator under the squared error loss function is given by the corresponding posterior mean. Accordingly, the Bayes estimate, denoted by $\tilde{\psi}(\boldsymbol{\theta})$, can be expressed as

$$\tilde{\psi}(\boldsymbol{\theta}) = \int_0^{\infty}\int_0^{\infty}\psi(\boldsymbol{\theta})\,G_1(\boldsymbol{\theta}|\underline{\mathrm{x}}, \mathbf{s})\,d\mu\,d\sigma, \quad (3.6)$$

where $G_1(\boldsymbol{\theta}|\underline{\mathrm{x}}, \mathbf{s})$ denotes the joint posterior distribution of $\boldsymbol{\theta}$ provided in (3.3).

It is evident that the Bayes estimator in (3.6) involves multidimensional integrals with respect to the joint posterior distribution, which are analytically intractable due to the complex form of the likelihood structure. Although direct numerical integration or standard Monte Carlo methods could, in principle, be applied, such approaches become computationally burdensome and inefficient in this setting. To overcome these difficulties, we employ the MCMC techniques to generate samples from the posterior distribution in (3.3). These simulated samples provide a practical and reliable means for approximating the Bayes estimates as well as constructing the corresponding BCIs. Implementation of the MCMC procedure requires the derivation of the full conditional distributions of the unknown parameters. Based on the joint posterior distribution in (3.3), the conditional densities of μ and σ can be expressed as follows:

$$\begin{aligned} G_1(\mu|\sigma, \underline{\mathrm{x}}, \mathbf{s}) \;\propto\;& \mu^{m+\tau_1-1} \exp\left\{(\sigma-1)\sum_{i=1}^{m} \log(1+\mu x_i) - \sum_{i=1}^{m}(1+\mu x_i)^{\sigma}\right. \\ &+ \left.\sum_{i=1}^{k} S_i \log\left[1-e^{1-(1+\mu x_i)^{\sigma}}\right] + S_m \log\left[1-e^{1-(1+\mu x_m)^{\sigma}}\right] - \epsilon_1\mu\right\} \end{aligned} \tag{3.7}$$

and

$$\begin{aligned} G_1(\sigma|\mu, \underline{\mathrm{x}}, \mathbf{s}) \;\propto\;& \sigma^{m+\tau_2-1} \exp\left\{\sigma\sum_{i=1}^{m} \log(1+\mu x_i) - \sum_{i=1}^{m}(1+\mu x_i)^{\sigma}\right. \\ &+ \left.\sum_{i=1}^{k} S_i \log\left[1-e^{1-(1+\mu x_i)^{\sigma}}\right] + S_m \log\left[1-e^{1-(1+\mu x_m)^{\sigma}}\right] - \epsilon_2\sigma\right\}. \end{aligned} \tag{3.8}$$

Inspection of the full conditional densities in (3.7) and (3.8) reveals that they do not correspond to any standard probability distributions. Consequently, direct sampling from these conditionals is not feasible using conventional methods. To circumvent this difficulty, a Metropolis–Hastings (M–H) step is embedded within the MCMC scheme to generate samples from the target posterior distribution. The implementation of the M–H procedure requires specifying appropriate proposal distributions. In this study, we adopt normal proposal distributions for μ and σ, with their means and variances determined based on the corresponding MLEs. This choice facilitates efficient exploration of the parameter space and improves the convergence behavior of the Markov chain. Since the model parameters are defined over the positive real line, the support of the proposal mechanism must respect this constraint. Accordingly, any candidate values generated from the normal proposal distributions that fall outside the admissible domain are discarded within the M–H step. The procedure for generating posterior samples using the M–H algorithm is summarized as follows.

Step 1. Initialize the Markov chain by setting $(\mu^{(0)}, \sigma^{(0)}) = (\hat{\mu}, \hat{\sigma})$.

Step 2. Set the iteration index $j = 1$.

Step 3. Update μ given $\sigma^{(j-1)}$ using an M–H step:

- Generate a candidate value μ^* from the normal proposal distribution $N(\mu^{(j-1)}, \widehat{\mathrm{var}}(\hat{\mu}))$.

- Compute the acceptance probability

$$\text{AP} = \min\left\{1,\ \frac{G_1(\mu^* \mid \sigma^{(j-1)}, \underline{\mathbf{x}}, \mathbf{s})}{G_1(\mu^{(j-1)} \mid \sigma^{(j-1)}, \underline{\mathbf{x}}, \mathbf{s})}\right\}.$$

- Generate $u \sim U(0, 1)$.
- Set $\mu^{(j)} = \mu^*$ if $u \leq \text{AP}$; otherwise, set $\mu^{(j)} = \mu^{(j-1)}$.

Step 4. Update σ given $\mu^{(j)}$ using a similar M–H step based on the conditional distribution in (3.8).

Step 5. Using the updated values $(\mu^{(j)}, \sigma^{(j)})$, compute the RF and HRF at time t as

$$R^{(j)} = 1 - \exp\left\{1 - \left(1 + \frac{\mu^{(j)}}{t}\right)^{\sigma^{(j)}}\right\},$$

and

$$h^{(j)} = \mu^{(j)}\sigma^{(j)}t^{-2}\left(1 + \frac{\mu^{(j)}}{t}\right)^{\sigma^{(j)}-1}\left[\exp\left\{\left(1 + \frac{\mu^{(j)}}{t}\right)^{\sigma^{(j)}} - 1\right\} - 1\right]^{-1}.$$

Step 6. Set $j = j + 1$ and repeat Steps 3–5 until a sufficiently large number of iterations is obtained.

Step 7. Discard the initial B iterations as burn-in to ensure convergence, and retain the remaining N samples:

$$\left\{\mu^{(j)}, \sigma^{(j)}, R^{(j)}, h^{(j)}\right\}, \quad j = 1, \ldots, N.$$

Once the posterior samples are generated via the MCMC procedure, they can be directly utilized to approximate the Bayes estimates and to construct the corresponding BCIs for the model parameters as well as the associated reliability measures. Under the squared error loss function, the Bayes estimates are given by the posterior means, which can be approximated using the retained MCMC samples as follows:

$$\tilde{\mu} = \frac{1}{N}\sum_{j=1}^{N}\mu^{(j)}, \quad \tilde{\sigma} = \frac{1}{N}\sum_{j=1}^{N}\sigma^{(j)}, \quad \tilde{R}(t) = \frac{1}{N}\sum_{j=1}^{N}R^{(j)}, \quad \text{and} \quad \tilde{h}(t) = \frac{1}{N}\sum_{j=1}^{N}h^{(j)}.$$

To construct the $100(1-\alpha)\%$ BCIs, the following procedure is adopted:

1. Sort the MCMC samples in ascending order for each quantity of interest, yielding

$$\left\{\mu^{[1]} < \mu^{[2]} < \cdots < \mu^{[N]}\right\}, \quad \left\{\sigma^{[1]} < \sigma^{[2]} < \cdots < \sigma^{[N]}\right\},$$

$$\left\{R^{[1]}(t) < R^{[2]} < \cdots < R^{[N]}\right\}, \quad \text{and} \quad \left\{h^{[1]}(t) < h^{[2]} < \cdots < h^{[N]}\right\}.$$

2. The equal-tail BCIs are then obtained by selecting the empirical quantiles corresponding to the levels $\alpha/2$ and $1 - \alpha/2$, namely

$$\left\{\mu^{[\alpha N/2]}, \mu^{[N(1-\alpha/2)]}\right\}, \quad \left\{\sigma^{[\alpha N/2]}, \sigma^{[N(1-\alpha/2)]}\right\},$$

$$\left\{R^{[\alpha N/2]}, R^{[N(1-\alpha/2)]}\right\}, \quad \text{and} \quad \left\{h^{[\alpha N/2]}, h^{[N(1-\alpha/2)]}\right\}.$$

4. Simulation comparisons

To investigate the finite-sample performance of the proposed estimators for σ, μ, $R(t)$, $h(t)$, and ϕ, an extensive Monte Carlo simulation experiment was performed using 1000 APTIIC samples under random binomial removals; see Algorithm 1. Two INH populations were considered throughout the study, namely, Pop-1: INH$(0.8, 0.5)$ and Pop-2: INH$(2.0, 1.5)$. Several experimental settings were examined by varying the binomial removal proportion ϕ, the threshold value T, and the sample size n. In particular, the simulation configurations were generated for $\phi = (0.4, 0.8)$ and $n = (30, 50, 80)$, whereas the number of observed failures m was determined according to the realized failure pattern corresponding to each selected value of n.

To evaluate the role of the threshold parameter T in the inferential analysis, two different threshold levels were considered for each combination of ϕ, n, and m. More specifically, the choices $T = (0.5, 1.5)$ and $T = (3, 5)$ were adopted for Pop-1 and Pop-2, respectively. In addition, at $t = 0.1$ and $t = 1$, the corresponding true values of $(R(t), h(t))$ for Pop-1 and Pop-2 were taken as $(0.9589, 1.1966)$ and $(0.9947, 0.0396)$, respectively. To assess the impact of the joint prior distributions $g_1(\boldsymbol{\theta})$ and $g_2(\phi)$ on Bayesian estimation, informative hyperparameters $\tau_j > 0$ and $\epsilon_j > 0$ $(j = 1, 2)$ associated with the INH(σ, μ) model parameters were elicited using the prior elicitation approach proposed by Kundu [25]. Practically, following this approach, the values of parameters τ_j and ϵ_j for $j = 1, 2$ are specified in such a way that the mean of gamma priors produces the actual values of σ and μ, i.e., $\sigma = \frac{\tau_1}{\epsilon_1}$ and $\mu = \frac{\tau_2}{\epsilon_2}$. Accordingly, the hyperparameter combinations employed in the Bayesian computations are summarized below:

- For Pop-1:
  - Prior-1: $(4, 5, 2.5, 5, 4, 6)$;
  - Prior-2: $(8, 10, 5, 10, 8, 12)$.
- For Pop-2:
  - Prior-1: $(10, 5, 7.5, 5, 4, 6)$;
  - Prior-2: $(20, 10, 15, 10, 8, 12)$.

Furthermore, for both populations $(i = 1, 2)$, two informative beta prior settings were considered for the hyperparameters τ_3 and ϵ_3 associated with ϕ. The first prior setting (Prior-1) assumes $\tau_3 = (4, 8)$ and $\epsilon_3 = (6, 2)$, while the second prior setting (Prior-2) uses $\tau_3 = (8, 16)$ and $\epsilon_3 = (12, 4)$. To guarantee adequate convergence of the MCMC algorithm described in Section 3, the first 2000 iterations were discarded as burn-in samples. Thereafter, 12000 posterior draws were retained for computing the Bayesian point estimates together with the associated 95% BCIs of σ, μ, $R(t)$, $h(t)$, and ϕ. The initial values required for the MCMC procedure were chosen from the corresponding frequentist estimates.

All numerical analyses were conducted using R version 4.2.2. In particular, the frequentist optimization routines and Bayesian MCMC implementation were carried out through the maxLik package by Henningsen and Toomet [26] and the coda package by Plummer et al. [27], respectively. The Newton–Raphson algorithm was implemented with a maximum of 1000 iterations. Convergence was assumed when the absolute difference between two consecutive log-likelihood values fell below 10^{-6}. All numerical computations were performed on a standard personal laptop equipped with an Intel® Core™ i5-5200U processor (2.20 GHz), 8 GB RAM, and Intel® HD Graphics 5500, running a Windows operating system.

Algorithm 1 Generation Procedure for the APTIIC Scheme with Random Binomial Removals

Input: Specify the parameters σ, μ, ϕ, n, m, and T.

Generate the first removal number

$$s_1 \sim \mathrm{Bin}(n-m, \phi).$$

Generate the subsequent removal numbers

$$s_i \sim \mathrm{Bin}\left(n-m-\sum_{v=1}^{i-1} s_v,\ \phi\right),$$

for

$$i = \begin{cases} 2, 3, \ldots, m-1, & \text{if } X_m < T, \\ 2, 3, \ldots, k, & \text{if } X_m > T. \end{cases}$$

Generate independent random variables

$$Z_i \sim U(0,1), \qquad i = 1, 2, \ldots, m.$$

Compute

$$V_i = Z_i^{\left(i+\sum_{l=m-i+1}^{m} s_l\right)^{-1}}, \qquad i = 1, 2, \ldots, m.$$

Compute

$$U_i = 1 - \prod_{j=m-i+1}^{m} V_j, \qquad i = 1, 2, \ldots, m.$$

Obtain

$$X_i = F^{-1}(u_i; \sigma, \mu), \qquad i = 1, 2, \ldots, m.$$

Determine k at T.

if $T < X_m$ **then**

Set

$$s_m = n - m - \sum_{i=1}^{k} s_i.$$

else

Set

$$s_m = n - m - \sum_{i=1}^{m-1} s_i.$$

end if

Obtain

$$X_i = \frac{f(x)}{R(x_{k+1})}, \qquad i = k+2, \ldots, m.$$

Output: Observations of APTIIC with binomial removals from the INH model.

Moreover, to further assess the efficiency of the proposed MH sampler, the acceptance rates were computed for two APTIIC samples with random binomial removals generated from Pop-1 under Prior-

1, using the configuration $(m, n) = (10, 30)$ and $(\phi, T) = (0.4, 0.5)$ as a representative example. The resulting acceptance rates were approximately 68% and 72%, respectively. These values fall within the commonly recommended range for efficient MCMC sampling, indicating that the proposed MH algorithm achieves satisfactory mixing and effectively explores the posterior distribution.

To verify the convergence of the proposed MH algorithm, a series of standard MCMC diagnostic plots were examined using the 10000 posterior samples retained after removing the initial 2000 burn-in iterations. For illustrative purposes, Figure 1 presents the diagnostics for the parameters σ and μ, the reliability measures $R(t)$ and $h(t)$ at $t = 0.1$, together with the binomial parameter ϕ corresponding to INH$(0.8, 0.5)$ and $\phi = 0.4$. The ACF plots in Figure 1(i) show a rapid decay of autocorrelation as the lag increases, indicating that the posterior samples exhibit only weak serial dependence. The trace plots displayed in Figure 1(ii) fluctuate randomly around stable posterior means without noticeable trends or abrupt shifts, demonstrating satisfactory mixing of the Markov chains. Moreover, the ergodic mean plots in Figure 1(iii) converge to nearly constant values as the iterations progress, providing clear evidence that the generated chains have reached their stationary distributions. Taken together, these diagnostic results confirm the convergence and stability of the implemented MH algorithm and indicate that the resulting Bayesian estimates and associated credible intervals are highly reliable.

To evaluate the accuracy of the point estimators of ϕ (as an illustrative example), two commonly used performance measures, namely, the root mean squared error (RMSE) and the average relative absolute bias (ARAB), were employed. These measures are defined as

$$\text{RMSE}\left(\check{\phi}\right) = \sqrt{\frac{1}{1000}\sum_{i=1}^{1000}\left(\check{\phi}^{[i]} - \phi\right)^2}$$

and

$$\text{ARAB}\left(\check{\phi}\right) = \frac{1}{1000}\sum_{i=1}^{1000}\phi^{-1}\left|\check{\phi}^{[i]} - \phi\right|,$$

where $\check{\phi}^{[i]}$ represents the estimate of ϕ obtained from the ith simulated sample.

For interval estimation, two additional criteria, namely, the average interval length (AIL) and the coverage probability (CP), were considered. These measures are given by

$$\text{AIL}_{95\%}(\phi) = \frac{1}{1000}\sum_{i=1}^{1000}\left(\mathcal{U}_{\check{\phi}^{[i]}}(\phi) - \mathcal{L}_{\check{\phi}^{[i]}}(\phi)\right)$$

and

$$\text{CP}_{95\%}(\phi) = \frac{1}{1000}\sum_{i=1}^{1000}\mathsf{I}_{\left(\mathcal{L}_{\check{\phi}^{[i]}}(\phi),\,\mathcal{U}_{\check{\phi}^{[i]}}(\phi)\right)}(\phi),$$

where I denotes the indicator function, while $\mathcal{L}(\cdot)$ and $\mathcal{U}(\cdot)$ denote the corresponding lower and upper bounds of the 95% confidence (or credible) interval, respectively. The numerical findings corresponding to σ, μ, $R(t)$, $h(t)$, and ϕ are summarized in Tables 1–10. In particular, Tables 1–5 present the RMSE and ARAB values, whereas Tables 6–10 provide the AIL and CP results.

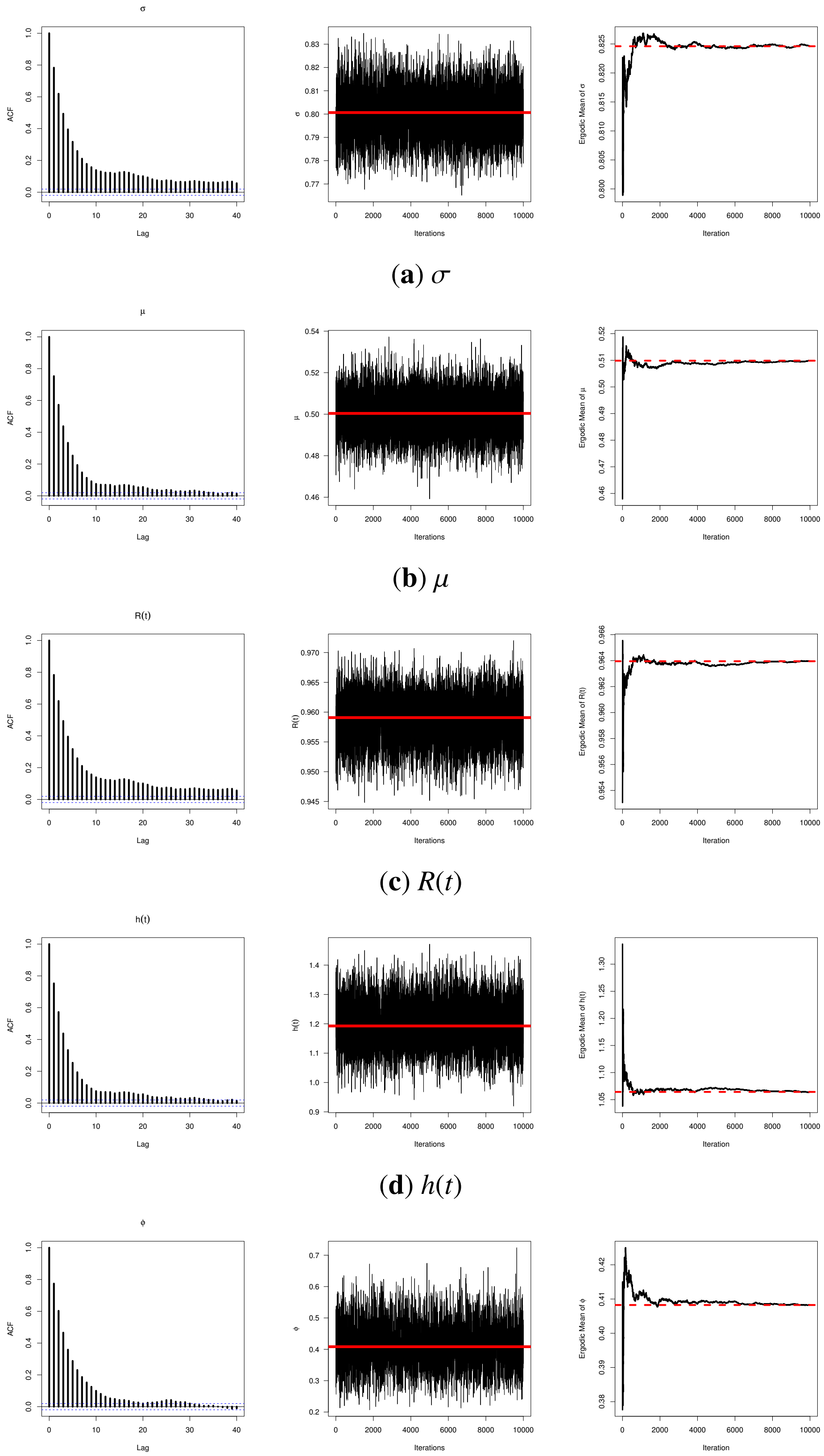

(**a**) σ

(**b**) μ

(**c**) $R(t)$

(**d**) $h(t)$

(**e**) ϕ

(i) ACF (ii) Trace (iii) Ergodic

Figure 1. Three convergence diagnostics for 10,000 MCMC iterations of σ, μ, $R(t)$, $h(t)$, and ϕ.

Based on smaller values of RMSE, ARAB, and AIL, together with larger CP values, the following observations can be made:

- The proposed inferential procedures produce accurate and stable estimates for σ, μ, $R(t)$, $h(t)$, and ϕ under the considered censoring framework.
- As the sample size n (or equivalently, the number of observed failures m) increases, both point and interval estimators exhibit improved performance.
- Bayesian point estimates and credible interval estimates associated with σ, μ, $R(t)$, $h(t)$, and ϕ generally outperform the corresponding frequentist estimators and asymptotic confidence intervals. This improvement can be attributed to the incorporation of informative gamma and beta prior distributions. This behavior can be attributed to the fact that Bayesian inference incorporates both the information contained in the observed sample and the available prior knowledge about the unknown parameters through the posterior distribution. Consequently, the resulting estimators are based on a richer source of information than the likelihood alone, leading to improved estimation accuracy, particularly for small and moderate sample sizes.
- As the censoring level increases, fewer failure observations are available, resulting in a loss of information and, consequently, larger estimation errors and variability for both estimation methods. Conversely, when the censoring intensity decreases or the sample size increases, the amount of available information becomes greater.
- For increasing values of ϕ in both Pop-1 and Pop-2, the following patterns are observed:
  - The RMSEs, ARABs, and AILs corresponding to μ and $R(t)$ tend to decrease, whereas those associated with σ, $h(t)$, and ϕ tend to increase;
  - The CP values for σ, $h(t)$, and ϕ decrease, while the CP values for μ and $R(t)$ increase.
- As the threshold parameter T increases for both populations, the RMSEs, ARABs, and AILs associated with all unknown parameters tend to decrease, indicating an improvement in estimation accuracy and interval precision. In contrast, the corresponding CP values exhibit an increasing trend.
- An increase in the threshold parameter T reduces the degree of censoring generated by the adaptive progressive scheme. Consequently, the observed sample contains more information, leading to lower estimator variability and improved inferential accuracy.
- When the parameter values of the INH(σ, μ) distribution increase, the following behaviors are observed:
  - The RMSEs and ARABs of σ increase, while those corresponding to μ, $R(t)$, and $h(t)$ decrease;
  - The AIL values for μ, $R(t)$, and $h(t)$ narrow down, whereas those for σ increase;
  - The CP values associated with σ decrease, while those corresponding to μ, $R(t)$, and $h(t)$ increase.
- The empirical coverage probabilities obtained from both ACIs and BCIs remain reasonably close to the nominal confidence level of 95%.
- Overall, the Bayesian framework based on MCMC implementation with independent gamma and beta informative priors is recommended for lifetime inference under the INH distribution when the data are collected through an APTIIC scheme with random binomial removals.

Table 1. The RMSE (1st Col.) and ARAB (2nd Col.) of σ.

(m,n)	MLE		Bayes[Prior-1]		Bayes[Prior-2]		MLE		Bayes[Prior-1]		Bayes[Prior-2]	
Pop-1												
$(\phi, T) \rightarrow$			(0.4,0.5)						(0.4,1.5)			
(10,30)	1.5685	0.9733	0.5117	0.3968	0.2817	0.1998	1.1861	0.7742	0.4502	0.3568	0.2697	0.1908
(20,30)	1.1554	0.7376	0.2754	0.2458	0.1998	0.1518	0.8877	0.6915	0.2646	0.2451	0.1949	0.1384
(20,50)	0.5113	0.3011	0.2173	0.1856	0.1717	0.1274	0.3620	0.2230	0.1867	0.1800	0.1524	0.1224
(40,50)	0.1673	0.1625	0.1529	0.1487	0.1337	0.1012	0.1647	0.1559	0.1512	0.1366	0.1170	0.0609
(30,80)	0.1556	0.1497	0.1377	0.1180	0.0398	0.0294	0.1510	0.1462	0.1274	0.1128	0.0338	0.0199
(60,80)	0.1384	0.1292	0.1233	0.1047	0.0231	0.0138	0.1316	0.1263	0.1213	0.1038	0.0213	0.0123
$(\phi, T) \rightarrow$			(0.8,0.5)						(0.8,1.5)			
(10,30)	1.3851	0.8301	0.4200	0.3726	0.2689	0.1612	0.9705	0.7458	0.3885	0.3500	0.2523	0.1487
(20,30)	0.9915	0.5400	0.2750	0.2449	0.1803	0.1366	0.7277	0.5246	0.2612	0.2328	0.1725	0.1233
(20,50)	0.3831	0.2130	0.1818	0.1627	0.1506	0.1251	0.2590	0.1928	0.1731	0.1596	0.1417	0.1210
(40,50)	0.1610	0.1519	0.1384	0.1334	0.1066	0.0468	0.1558	0.1483	0.1364	0.1275	0.0657	0.0432
(30,80)	0.1451	0.1433	0.1267	0.1105	0.0338	0.0217	0.1444	0.1391	0.1240	0.1069	0.0315	0.0190
(60,80)	0.1243	0.1200	0.1158	0.0948	0.0206	0.0113	0.1212	0.1169	0.1122	0.0907	0.0187	0.0105
Pop-2												
$(\phi, T) \rightarrow$			(0.4,3)						(0.4,5)			
(10,30)	1.6407	1.4534	0.6399	0.4140	0.2920	0.2290	1.5411	0.7716	0.5003	0.3577	0.2752	0.2187
(20,30)	1.2867	0.7862	0.5546	0.2631	0.2529	0.1908	1.1531	0.5884	0.4776	0.2581	0.2266	0.1798
(20,50)	0.6038	0.4217	0.3598	0.2438	0.2230	0.1518	0.4385	0.3892	0.2813	0.2401	0.2144	0.1464
(40,50)	0.3500	0.2590	0.2101	0.1798	0.1556	0.1126	0.2799	0.2540	0.1856	0.1599	0.1524	0.1091
(30,80)	0.2173	0.2113	0.1713	0.1460	0.1243	0.1073	0.2130	0.1925	0.1462	0.1245	0.1200	0.0986
(60,80)	0.1559	0.1464	0.1222	0.1124	0.0978	0.0482	0.1512	0.1337	0.1177	0.1051	0.0716	0.0299
$(\phi, T) \rightarrow$			(0.8,3)						(0.8,5)			
(10,30)	1.4394	1.3051	0.6038	0.3885	0.2776	0.2096	1.3511	0.7606	0.4903	0.3508	0.2672	0.2064
(20,30)	1.1393	0.6031	0.5242	0.2455	0.2401	0.1612	0.8375	0.5549	0.3657	0.2432	0.2158	0.1552
(20,50)	0.5549	0.3620	0.3011	0.2300	0.1928	0.1402	0.3802	0.3577	0.2630	0.2227	0.1867	0.1375
(40,50)	0.2340	0.2291	0.1861	0.1692	0.1444	0.1076	0.2297	0.1949	0.1746	0.1584	0.1402	0.0992
(30,80)	0.2095	0.1625	0.1552	0.1204	0.1100	0.1008	0.1731	0.1596	0.1451	0.1170	0.1039	0.0967
(60,80)	0.1240	0.1166	0.0927	0.0701	0.0657	0.0338	0.1321	0.0997	0.0906	0.0674	0.0375	0.0190

Table 2. The RMSE (1st Col.) and ARAB (2nd Col.) of μ.

(m,n)	MLE		Bayes[Prior-1]		Bayes[Prior-2]		MLE		Bayes[Prior-1]		Bayes[Prior-2]	
Pop-1												
$(\phi,T)\rightarrow$			(0.4,0.5)						(0.4,1.5)			
(10,30)	1.1353	0.7358	0.4979	0.3986	0.3530	0.3105	0.9372	0.5823	0.4758	0.3845	0.3106	0.2120
(20,30)	0.7824	0.4825	0.4114	0.3440	0.2919	0.2072	0.6375	0.4074	0.3984	0.3168	0.2346	0.1995
(20,50)	0.5889	0.4611	0.3288	0.2673	0.2419	0.1807	0.4969	0.3631	0.3154	0.2579	0.2048	0.1397
(40,50)	0.4972	0.3640	0.3058	0.2124	0.2011	0.1314	0.4657	0.3246	0.2848	0.2057	0.1874	0.1312
(30,80)	0.4042	0.2898	0.2608	0.1920	0.1661	0.1253	0.3984	0.2828	0.2403	0.1721	0.1646	0.1029
(60,80)	0.3256	0.2674	0.2252	0.1792	0.1566	0.1112	0.3210	0.2314	0.2114	0.1571	0.1448	0.0970
$(\phi,T)\rightarrow$			(0.8,0.5)						(0.8,1.5)			
(10,30)	1.2949	0.8135	0.5823	0.4702	0.3874	0.3168	1.0209	0.7601	0.5285	0.4683	0.3315	0.2466
(20,30)	0.9812	0.6779	0.4657	0.3818	0.2977	0.2167	0.8211	0.5215	0.4456	0.3445	0.2795	0.2119
(20,50)	0.6012	0.4623	0.3564	0.3106	0.2466	0.1973	0.5526	0.3755	0.3295	0.2763	0.2053	0.1510
(40,50)	0.5683	0.4429	0.3067	0.2448	0.2171	0.1481	0.4758	0.3285	0.3065	0.2412	0.1892	0.1359
(30,80)	0.4498	0.3567	0.2890	0.2124	0.1941	0.1258	0.4233	0.2922	0.2837	0.2056	0.1697	0.1203
(60,80)	0.3533	0.2827	0.2517	0.1845	0.1600	0.1231	0.3486	0.2550	0.2220	0.1646	0.1459	0.1013
Pop-2												
$(\phi,T)\rightarrow$			(0.4,3)						(0.4,5)			
(10,30)	0.8920	0.5670	0.4671	0.4429	0.3142	0.2454	0.7771	0.5153	0.4658	0.3818	0.2480	0.2011
(20,30)	0.7520	0.4498	0.3699	0.3163	0.2754	0.1819	0.4545	0.4284	0.3637	0.2961	0.2079	0.1792
(20,50)	0.4050	0.3580	0.2781	0.2541	0.2119	0.1646	0.3766	0.3293	0.2754	0.2140	0.1662	0.1171
(40,50)	0.3851	0.2848	0.2705	0.1973	0.1546	0.0841	0.3107	0.2820	0.2026	0.1944	0.1304	0.0830
(30,80)	0.2608	0.2517	0.2048	0.1660	0.1248	0.0656	0.2579	0.2408	0.1768	0.1258	0.1040	0.0635
(60,80)	0.2310	0.2052	0.1448	0.1112	0.1029	0.0507	0.2163	0.1571	0.1375	0.1053	0.0866	0.0488
$(\phi,T)\rightarrow$			(0.8,3)						(0.8,5)			
(10,30)	1.1812	0.7678	0.5522	0.5015	0.3526	0.2525	0.9372	0.6779	0.4806	0.3874	0.2878	0.2214
(20,30)	0.8211	0.5522	0.4448	0.3258	0.3062	0.2056	0.6808	0.5092	0.3964	0.3121	0.2370	0.1941
(20,50)	0.5808	0.4042	0.3370	0.2827	0.2212	0.1671	0.4478	0.3924	0.2905	0.2550	0.1721	0.1388
(40,50)	0.3909	0.3254	0.2759	0.2092	0.1600	0.1199	0.3415	0.3065	0.2314	0.1995	0.1484	0.0922
(30,80)	0.3530	0.2693	0.2072	0.1873	0.1305	0.0791	0.2890	0.2674	0.1946	0.1397	0.1082	0.0737
(60,80)	0.2403	0.2303	0.1515	0.1231	0.1145	0.0555	0.2367	0.1646	0.1459	0.1203	0.0977	0.0510

Table 3. The RMSE (1st Col.) and ARAB (2nd Col.) of $R(t)$.

(m,n)	MLE		Bayes[Prior-1]		Bayes[Prior-2]		MLE		Bayes[Prior-1]		Bayes[Prior-2]	
Pop-1												
$(\phi,T)\rightarrow$			(0.4,0.5)						(0.4,1.5)			
(10,30)	0.9315	0.8076	0.7469	0.6953	0.3753	0.3195	0.8218	0.8029	0.6989	0.6335	0.3216	0.2731
(20,30)	0.7613	0.6300	0.5180	0.3977	0.3385	0.3056	0.6409	0.5240	0.4282	0.3513	0.3056	0.2538
(20,50)	0.4990	0.4245	0.3957	0.3164	0.2503	0.1998	0.4524	0.3974	0.3766	0.2938	0.2373	0.1947
(40,50)	0.3953	0.3465	0.2327	0.2186	0.1935	0.1913	0.3617	0.3058	0.2233	0.2090	0.1924	0.1876
(30,80)	0.2449	0.2209	0.2031	0.1964	0.1846	0.1734	0.2305	0.2150	0.2028	0.1891	0.1768	0.1707
(60,80)	0.2021	0.1929	0.1841	0.1662	0.1619	0.1580	0.1944	0.1915	0.1690	0.1640	0.1582	0.1445
$(\phi,T)\rightarrow$			(0.8,0.5)						(0.8,1.5)			
(10,30)	0.9217	0.7930	0.7249	0.6721	0.3706	0.3090	0.8017	0.7814	0.6754	0.6135	0.3112	0.2596
(20,30)	0.7580	0.6268	0.4375	0.3377	0.3253	0.2832	0.6351	0.5237	0.4266	0.3334	0.3033	0.2477
(20,50)	0.4745	0.4014	0.3528	0.3081	0.2411	0.1961	0.4281	0.3855	0.3332	0.2568	0.2333	0.1927
(40,50)	0.3842	0.3347	0.2293	0.2181	0.1912	0.1860	0.3579	0.3016	0.2214	0.2032	0.1904	0.1813
(30,80)	0.2442	0.2198	0.1976	0.1954	0.1787	0.1689	0.2294	0.2128	0.1967	0.1875	0.1759	0.1645
(60,80)	0.1962	0.1893	0.1834	0.1641	0.1581	0.1536	0.1932	0.1853	0.1662	0.1622	0.1576	0.1438
Pop-2												
$(\phi,T)\rightarrow$			(0.4,3)						(0.4,5)			
(10,30)	0.4956	0.4282	0.3947	0.3385	0.2503	0.1998	0.4720	0.3974	0.3509	0.3164	0.2333	0.1947
(20,30)	0.4266	0.3266	0.2693	0.2437	0.2186	0.1913	0.3508	0.3057	0.2505	0.2209	0.2089	0.1846
(20,50)	0.2449	0.2294	0.2114	0.1935	0.1768	0.1213	0.2327	0.2171	0.1964	0.1875	0.1561	0.0785
(40,50)	0.2377	0.1857	0.1548	0.1077	0.0845	0.0699	0.2128	0.1690	0.1273	0.0965	0.0754	0.0555
(30,80)	0.1962	0.1636	0.0885	0.0695	0.0492	0.0456	0.1853	0.1536	0.0702	0.0577	0.0490	0.0392
(60,80)	0.1421	0.1074	0.0647	0.0476	0.0402	0.0341	0.1354	0.1053	0.0614	0.0470	0.0363	0.0304
$(\phi,T)\rightarrow$			(0.8,3)						(0.8,5)			
(10,30)	0.4282	0.3825	0.3081	0.2575	0.2411	0.1961	0.3855	0.3377	0.3070	0.2442	0.2214	0.1924
(20,30)	0.4251	0.2954	0.2388	0.2229	0.2181	0.1891	0.3489	0.2826	0.2305	0.2198	0.1904	0.1787
(20,50)	0.2442	0.2267	0.1954	0.1825	0.1320	0.1030	0.2293	0.2150	0.1912	0.1759	0.1105	0.0739
(40,50)	0.2021	0.1662	0.1547	0.0986	0.0805	0.0654	0.1915	0.1580	0.1036	0.0960	0.0688	0.0544
(30,80)	0.1905	0.1485	0.0766	0.0668	0.0481	0.0447	0.1494	0.1180	0.0673	0.0539	0.0450	0.0378
(60,80)	0.1318	0.0977	0.0630	0.0462	0.0392	0.0339	0.1257	0.0956	0.0568	0.0447	0.0350	0.0300

Table 4. The RMSE (1st Col.) and ARAB (2nd Col.) of $h(t)$.

(m,n)	MLE		Bayes[Prior-1]		Bayes[Prior-2]		MLE		Bayes[Prior-1]		Bayes[Prior-2]	
Pop-1												
$(\phi,T)\rightarrow$			(0.4,0.5)						(0.4,1.5)			
(10,30)	1.1353	0.7358	0.4979	0.3986	0.3530	0.2454	0.9372	0.5823	0.4758	0.3845	0.3106	0.2202
(20,30)	0.7824	0.4825	0.4114	0.3440	0.2919	0.2072	0.6375	0.4074	0.3984	0.3168	0.2346	0.1995
(20,50)	0.5889	0.4611	0.3288	0.2673	0.2419	0.1807	0.4969	0.3631	0.3154	0.2579	0.2048	0.1397
(40,50)	0.4972	0.3640	0.3058	0.2124	0.2011	0.1314	0.4657	0.3246	0.2848	0.2057	0.1874	0.1312
(30,80)	0.4042	0.2898	0.2608	0.1920	0.1661	0.1253	0.3984	0.2828	0.2403	0.1721	0.1646	0.1029
(60,80)	0.3256	0.2674	0.2252	0.1792	0.1566	0.1112	0.3210	0.2314	0.2114	0.1571	0.1448	0.0970
$(\phi,T)\rightarrow$			(0.8,0.5)						(0.8,1.5)			
(10,30)	1.2949	0.8135	0.5823	0.4702	0.3874	0.2525	1.0209	0.7601	0.5285	0.4683	0.3315	0.2214
(20,30)	1.0812	0.6779	0.4657	0.3818	0.2977	0.2167	0.8211	0.5215	0.4456	0.3445	0.2795	0.2119
(20,50)	0.6012	0.4623	0.3370	0.3106	0.2466	0.1973	0.5526	0.3755	0.3295	0.2763	0.2053	0.1510
(40,50)	0.5683	0.4429	0.3067	0.2448	0.2171	0.1481	0.4758	0.3285	0.3065	0.2412	0.1892	0.1359
(30,80)	0.4498	0.3567	0.2890	0.2124	0.1941	0.1258	0.4233	0.2922	0.2837	0.2056	0.1697	0.1203
(60,80)	0.3533	0.2827	0.2517	0.1845	0.1600	0.1231	0.3486	0.2550	0.2220	0.1646	0.1459	0.1013
Pop-2												
$(\phi,T)\rightarrow$			(0.4,3)						(0.4,5)			
(10,30)	0.8920	0.5670	0.4671	0.3925	0.3142	0.3105	0.7771	0.5153	0.4658	0.3818	0.2480	0.2011
(20,30)	0.7520	0.4498	0.3699	0.3163	0.2754	0.1819	0.4545	0.4284	0.3637	0.2961	0.2079	0.1792
(20,50)	0.4050	0.3580	0.2781	0.2541	0.2119	0.1646	0.3766	0.3293	0.2754	0.2140	0.1662	0.1171
(40,50)	0.3851	0.2848	0.2705	0.1973	0.1546	0.0841	0.3107	0.2820	0.2026	0.1944	0.1304	0.0830
(30,80)	0.2608	0.2517	0.2048	0.1660	0.1248	0.0656	0.2579	0.2408	0.1768	0.1258	0.1040	0.0635
(60,80)	0.2310	0.2052	0.1448	0.1112	0.1029	0.0507	0.2163	0.1571	0.1375	0.1053	0.0866	0.0488
$(\phi,T)\rightarrow$			(0.8,3)						(0.8,5)			
(10,30)	1.2812	0.7678	0.5522	0.4501	0.3526	0.3168	0.9372	0.6779	0.4806	0.3874	0.2878	0.2466
(20,30)	0.8211	0.5522	0.4448	0.3258	0.3062	0.2056	0.6808	0.5092	0.3964	0.3121	0.2370	0.1941
(20,50)	0.5808	0.4042	0.3564	0.2827	0.2212	0.1671	0.4478	0.3924	0.2905	0.2550	0.1721	0.1388
(40,50)	0.3909	0.3254	0.2759	0.2092	0.1600	0.1199	0.3415	0.3065	0.2314	0.1995	0.1484	0.0922
(30,80)	0.3530	0.2693	0.2072	0.1873	0.1305	0.0791	0.2890	0.2674	0.1946	0.1397	0.1082	0.0737
(60,80)	0.2403	0.2303	0.1515	0.1231	0.1145	0.0555	0.2367	0.1646	0.1459	0.1203	0.0977	0.0510

Table 5. The RMSE (1st Col.) and ARAB (2nd Col.) of ϕ from Pop-i ($i = 1, 2$).

(m,n)	MLE		Bayes[Prior-1]		Bayes[Prior-2]		MLE		Bayes[Prior-1]		Bayes[Prior-2]	
$T\rightarrow$			(0.5,1.5)						(3,5)			
$\phi = 0.4$												
(10,30)	0.2975	0.2408	0.1796	0.1544	0.1250	0.0861	0.2486	0.2053	0.1738	0.1270	0.1216	0.0754
(20,30)	0.2397	0.2005	0.1610	0.1518	0.1198	0.0845	0.2099	0.1904	0.1566	0.1112	0.1055	0.0859
(20,50)	0.2295	0.1680	0.1404	0.1255	0.0878	0.0725	0.1881	0.1444	0.1355	0.0903	0.0875	0.0661
(40,50)	0.2150	0.1603	0.1336	0.1230	0.0871	0.0696	0.1781	0.1365	0.1264	0.0898	0.0849	0.0630
(30,80)	0.1468	0.1254	0.1191	0.0836	0.0697	0.0636	0.1362	0.1251	0.0883	0.0700	0.0689	0.0603
(60,80)	0.1103	0.1049	0.0946	0.0658	0.0589	0.0500	0.1069	0.1019	0.0658	0.0592	0.0530	0.0484
$\phi = 0.8$												
(10,30)	0.3059	0.2476	0.2150	0.1787	0.1332	0.1092	0.2559	0.2288	0.2111	0.1513	0.1286	0.1039
(20,30)	0.2482	0.2044	0.1784	0.1404	0.1104	0.0916	0.2316	0.1759	0.1596	0.1250	0.1147	0.0737
(20,50)	0.2393	0.1751	0.1464	0.1308	0.0915	0.0756	0.1961	0.1505	0.1412	0.0942	0.0913	0.0689
(40,50)	0.2248	0.1658	0.1412	0.1271	0.0901	0.0720	0.1851	0.1419	0.1307	0.0929	0.0878	0.0651
(30,80)	0.1490	0.1273	0.1203	0.0849	0.0702	0.0644	0.1371	0.1268	0.0897	0.0710	0.0700	0.0610
(60,80)	0.1346	0.1280	0.1154	0.0802	0.0719	0.0611	0.1305	0.1244	0.0802	0.0722	0.0647	0.0591

Table 6. The AIL (1st Col.) and CP (2nd Col.) of σ.

(m,n)	ACI		BCI[Prior-1]		BCI[Prior-2]		ACI		BCI[Prior-1]		BCI[Prior-2]	
$T\rightarrow$			(0.5,1.5)						(3,5)			
$\phi=0.4$												
(10,30)	1.026	0.926	0.512	0.954	0.229	0.969	0.818	0.937	0.450	0.957	0.219	0.970
(20,30)	0.673	0.945	0.246	0.968	0.191	0.971	0.554	0.952	0.245	0.968	0.180	0.972
(20,50)	0.362	0.962	0.217	0.970	0.152	0.973	0.223	0.969	0.152	0.973	0.146	0.974
(40,50)	0.165	0.973	0.156	0.973	0.134	0.974	0.163	0.973	0.137	0.974	0.117	0.975
(30,80)	0.156	0.973	0.118	0.975	0.040	0.979	0.146	0.974	0.113	0.975	0.029	0.980
(60,80)	0.134	0.974	0.105	0.976	0.021	0.980	0.126	0.975	0.104	0.976	0.012	0.981
$(\phi,T)\rightarrow$			(0.8,0.5)						(0.8,1.5)			
(10,30)	0.794	0.939	0.420	0.959	0.210	0.970	0.643	0.947	0.373	0.961	0.206	0.970
(20,30)	0.439	0.958	0.245	0.968	0.161	0.973	0.299	0.965	0.233	0.969	0.155	0.973
(20,50)	0.213	0.970	0.173	0.972	0.140	0.974	0.193	0.971	0.142	0.974	0.137	0.974
(40,50)	0.161	0.973	0.133	0.974	0.107	0.976	0.148	0.974	0.128	0.975	0.066	0.978
(30,80)	0.145	0.974	0.111	0.976	0.032	0.980	0.144	0.974	0.107	0.976	0.022	0.980
(60,80)	0.117	0.975	0.095	0.976	0.019	0.981	0.112	0.975	0.091	0.977	0.010	0.981
Pop-2												
$(\phi,T)\rightarrow$			(0.4,3)						(0.4,5)			
(10,30)	1.369	0.923	0.772	0.949	0.282	0.970	1.169	0.932	0.568	0.957	0.243	0.971
(20,30)	1.055	0.937	0.555	0.958	0.258	0.971	0.853	0.945	0.263	0.971	0.182	0.974
(20,50)	0.709	0.951	0.281	0.970	0.223	0.972	0.438	0.963	0.240	0.972	0.133	0.976
(40,50)	0.467	0.962	0.180	0.974	0.152	0.975	0.254	0.971	0.156	0.975	0.109	0.977
(30,80)	0.362	0.966	0.171	0.974	0.120	0.977	0.217	0.972	0.124	0.976	0.099	0.978
(60,80)	0.163	0.975	0.146	0.976	0.105	0.977	0.156	0.975	0.112	0.977	0.072	0.979
$(\phi,T)\rightarrow$			(0.8,0.5)						(0.8,1.5)			
(10,30)	1.148	0.932	0.761	0.949	0.278	0.970	0.985	0.940	0.435	0.963	0.216	0.973
(20,30)	0.834	0.946	0.524	0.959	0.240	0.972	0.749	0.950	0.243	0.971	0.154	0.975
(20,50)	0.531	0.959	0.263	0.971	0.193	0.974	0.380	0.965	0.230	0.972	0.125	0.976
(40,50)	0.389	0.965	0.175	0.974	0.140	0.976	0.234	0.972	0.144	0.976	0.099	0.978
(30,80)	0.213	0.973	0.155	0.975	0.110	0.977	0.173	0.974	0.117	0.977	0.097	0.978
(60,80)	0.145	0.976	0.107	0.977	0.070	0.979	0.134	0.976	0.100	0.978	0.066	0.979

Table 7. The AIL (1st Col.) and CP (2nd Col.) of μ.

(m,n)	ACI		BCI[Prior-1]		BCI[Prior-2]		ACI		BCI[Prior-1]		BCI[Prior-2]	
$T \rightarrow$			(0.5,1.5)						(3,5)			
$\phi = 0.4$												
(10,30)	0.736	0.938	0.467	0.956	0.353	0.964	0.582	0.948	0.399	0.960	0.248	0.971
(20,30)	0.637	0.945	0.364	0.963	0.292	0.968	0.483	0.955	0.317	0.966	0.200	0.974
(20,50)	0.497	0.954	0.315	0.966	0.258	0.970	0.461	0.957	0.267	0.970	0.181	0.975
(40,50)	0.466	0.956	0.285	0.968	0.206	0.974	0.364	0.963	0.212	0.973	0.131	0.979
(30,80)	0.398	0.961	0.261	0.970	0.165	0.977	0.290	0.968	0.172	0.976	0.110	0.980
(60,80)	0.321	0.966	0.225	0.972	0.147	0.978	0.267	0.970	0.157	0.977	0.097	0.981
$(\phi, T) \rightarrow$			(0.8,0.5)						(0.8,1.5)			
(10,30)	0.814	0.933	0.552	0.951	0.468	0.956	0.760	0.937	0.470	0.956	0.288	0.968
(20,30)	0.678	0.942	0.445	0.958	0.298	0.968	0.521	0.953	0.396	0.961	0.237	0.972
(20,50)	0.553	0.950	0.329	0.965	0.276	0.969	0.462	0.957	0.311	0.967	0.197	0.974
(40,50)	0.476	0.956	0.306	0.967	0.241	0.971	0.443	0.958	0.245	0.971	0.148	0.978
(30,80)	0.423	0.959	0.284	0.968	0.206	0.974	0.357	0.964	0.212	0.973	0.120	0.979
(60,80)	0.353	0.964	0.252	0.971	0.160	0.977	0.283	0.969	0.165	0.976	0.101	0.981
Pop-2												
$(\phi, T) \rightarrow$			(0.4,3)						(0.4,5)			
(10,30)	0.567	0.949	0.428	0.958	0.314	0.966	0.515	0.953	0.380	0.961	0.242	0.970
(20,30)	0.454	0.957	0.359	0.963	0.235	0.971	0.428	0.958	0.285	0.968	0.182	0.974
(20,50)	0.405	0.960	0.278	0.968	0.165	0.976	0.358	0.963	0.214	0.972	0.117	0.979
(40,50)	0.385	0.961	0.271	0.969	0.130	0.978	0.285	0.968	0.197	0.973	0.084	0.981
(30,80)	0.261	0.969	0.241	0.971	0.104	0.980	0.258	0.969	0.166	0.975	0.064	0.982
(60,80)	0.231	0.971	0.157	0.976	0.087	0.981	0.216	0.972	0.103	0.980	0.051	0.983
$(\phi, T) \rightarrow$			(0.8,3)						(0.8,5)			
(10,30)	0.768	0.936	0.524	0.952	0.331	0.965	0.678	0.942	0.428	0.958	0.285	0.968
(20,30)	0.552	0.950	0.419	0.959	0.280	0.968	0.509	0.953	0.293	0.967	0.206	0.973
(20,50)	0.448	0.957	0.283	0.968	0.172	0.975	0.392	0.961	0.221	0.972	0.139	0.977
(40,50)	0.391	0.961	0.276	0.968	0.148	0.977	0.306	0.966	0.200	0.973	0.092	0.980
(30,80)	0.353	0.963	0.267	0.969	0.108	0.979	0.269	0.969	0.187	0.974	0.079	0.981
(60,80)	0.237	0.971	0.165	0.976	0.098	0.980	0.230	0.971	0.120	0.978	0.053	0.983

Table 8. The AIL (1st Col.) and CP (2nd Col.) of $R(t)$.

(m, n)	ACI		BCI[Prior-1]		BCI[Prior-2]		ACI		BCI[Prior-1]		BCI[Prior-2]	
$T \rightarrow$			(0.5,1.5)						(3,5)			
$\phi = 0.4$												
(10,30)	0.931	0.930	0.803	0.939	0.375	0.968	0.808	0.938	0.695	0.946	0.322	0.972
(20,30)	0.518	0.958	0.398	0.967	0.338	0.971	0.428	0.965	0.351	0.970	0.306	0.973
(20,50)	0.397	0.967	0.316	0.972	0.250	0.977	0.396	0.967	0.294	0.974	0.200	0.980
(40,50)	0.233	0.978	0.209	0.980	0.191	0.981	0.219	0.979	0.194	0.981	0.188	0.981
(30,80)	0.203	0.980	0.196	0.980	0.173	0.982	0.203	0.980	0.177	0.982	0.171	0.982
(60,80)	0.194	0.981	0.166	0.982	0.162	0.983	0.193	0.981	0.164	0.983	0.145	0.984
$(\phi, T) \rightarrow$			(0.8,0.5)						(0.8,1.5)			
(10,30)	0.922	0.931	0.781	0.940	0.371	0.968	0.793	0.939	0.675	0.948	0.311	0.973
(20,30)	0.438	0.964	0.338	0.971	0.325	0.972	0.427	0.965	0.333	0.971	0.283	0.974
(20,50)	0.386	0.967	0.308	0.973	0.241	0.977	0.333	0.971	0.257	0.976	0.196	0.980
(40,50)	0.229	0.978	0.203	0.980	0.190	0.981	0.218	0.979	0.191	0.981	0.181	0.981
(30,80)	0.198	0.980	0.195	0.980	0.169	0.982	0.197	0.980	0.176	0.982	0.165	0.983
(60,80)	0.193	0.981	0.164	0.983	0.158	0.983	0.189	0.981	0.162	0.983	0.144	0.984
Pop-2												
$(\phi, T) \rightarrow$			(0.4,3)						(0.4,5)			
(10,30)	0.472	0.938	0.338	0.953	0.250	0.964	0.397	0.947	0.316	0.956	0.200	0.969
(20,30)	0.427	0.943	0.306	0.957	0.219	0.967	0.327	0.955	0.244	0.964	0.191	0.970
(20,50)	0.233	0.966	0.194	0.970	0.121	0.978	0.196	0.970	0.177	0.972	0.078	0.983
(40,50)	0.155	0.975	0.097	0.981	0.070	0.984	0.108	0.980	0.085	0.983	0.056	0.986
(30,80)	0.070	0.984	0.049	0.987	0.046	0.987	0.069	0.984	0.049	0.987	0.039	0.988
(60,80)	0.065	0.985	0.040	0.988	0.034	0.989	0.048	0.987	0.036	0.988	0.030	0.989
$(\phi, T) \rightarrow$			(0.8,3)						(0.8,5)			
(10,30)	0.428	0.943	0.338	0.953	0.241	0.965	0.386	0.948	0.308	0.957	0.196	0.970
(20,30)	0.425	0.943	0.283	0.960	0.218	0.967	0.295	0.958	0.223	0.967	0.190	0.970
(20,50)	0.229	0.966	0.191	0.970	0.111	0.980	0.195	0.970	0.176	0.972	0.074	0.984
(40,50)	0.155	0.975	0.096	0.981	0.069	0.985	0.104	0.981	0.081	0.983	0.054	0.986
(30,80)	0.067	0.985	0.048	0.987	0.045	0.987	0.067	0.985	0.045	0.987	0.038	0.988
(60,80)	0.063	0.985	0.039	0.988	0.034	0.989	0.046	0.987	0.035	0.988	0.030	0.989

Table 9. The AIL (1st Col.) and CP (2nd Col.) of $h(t)$.

(m,n)	ACI		BCI[Prior-1]		BCI[Prior-2]		ACI		BCI[Prior-1]		BCI[Prior-2]	
$T \rightarrow$			(0.5,1.5)						(3,5)			
$\phi = 0.4$												
(10,30)	0.736	0.941	0.476	0.958	0.353	0.966	0.582	0.951	0.399	0.963	0.248	0.972
(20,30)	0.637	0.947	0.398	0.963	0.292	0.969	0.483	0.957	0.317	0.968	0.200	0.975
(20,50)	0.497	0.956	0.315	0.968	0.258	0.972	0.461	0.959	0.267	0.971	0.181	0.977
(40,50)	0.466	0.958	0.285	0.970	0.206	0.975	0.364	0.965	0.212	0.975	0.131	0.980
(30,80)	0.398	0.963	0.261	0.971	0.165	0.978	0.290	0.970	0.172	0.977	0.103	0.982
(60,80)	0.321	0.968	0.225	0.974	0.157	0.979	0.267	0.971	0.157	0.978	0.097	0.983
$(\phi, T) \rightarrow$			(0.8,0.5)						(0.8,1.5)			
(10,30)	0.814	0.936	0.582	0.951	0.468	0.958	0.760	0.939	0.470	0.958	0.288	0.970
(20,30)	0.678	0.945	0.466	0.958	0.298	0.969	0.521	0.955	0.396	0.963	0.237	0.973
(20,50)	0.553	0.953	0.329	0.967	0.276	0.970	0.462	0.959	0.311	0.968	0.197	0.976
(40,50)	0.476	0.958	0.306	0.969	0.241	0.973	0.443	0.960	0.245	0.973	0.148	0.979
(30,80)	0.423	0.961	0.284	0.970	0.206	0.975	0.357	0.965	0.212	0.975	0.120	0.981
(60,80)	0.353	0.966	0.252	0.972	0.160	0.978	0.283	0.970	0.165	0.978	0.101	0.982
Pop-2												
$(\phi, T) \rightarrow$			(0.4,3)						(0.4,5)			
(10,30)	0.567	0.953	0.467	0.959	0.314	0.968	0.515	0.956	0.392	0.964	0.248	0.973
(20,30)	0.454	0.960	0.364	0.965	0.235	0.973	0.428	0.961	0.316	0.968	0.182	0.977
(20,50)	0.405	0.963	0.278	0.971	0.165	0.978	0.358	0.966	0.214	0.975	0.117	0.981
(40,50)	0.385	0.964	0.271	0.971	0.130	0.980	0.285	0.970	0.197	0.976	0.084	0.983
(30,80)	0.261	0.972	0.241	0.973	0.104	0.982	0.258	0.972	0.166	0.978	0.064	0.984
(60,80)	0.231	0.974	0.157	0.978	0.087	0.983	0.216	0.975	0.103	0.982	0.051	0.985
$(\phi, T) \rightarrow$			(0.8,3)						(0.8,5)			
(10,30)	0.768	0.940	0.552	0.954	0.331	0.967	0.678	0.946	0.419	0.962	0.285	0.970
(20,30)	0.552	0.954	0.445	0.960	0.280	0.971	0.509	0.956	0.326	0.968	0.206	0.975
(20,50)	0.448	0.960	0.283	0.970	0.172	0.977	0.392	0.964	0.221	0.974	0.139	0.979
(40,50)	0.391	0.964	0.276	0.971	0.148	0.979	0.306	0.969	0.200	0.976	0.092	0.982
(30,80)	0.353	0.966	0.267	0.971	0.108	0.981	0.269	0.971	0.187	0.976	0.079	0.983
(60,80)	0.237	0.973	0.165	0.978	0.098	0.982	0.230	0.974	0.120	0.981	0.053	0.985

Table 10. The AIL (1st Col.) and CP (2nd Col.) of ϕ.

(m,n)	ACI		BCI[Prior-1]		BCI[Prior-2]		ACI		BCI[Prior-1]		BCI[Prior-2]	
$T \rightarrow$			(0.5,1.5)						(3,5)			
$\phi = 0.4$												
(10,30)	0.224	0.947	0.168	0.960	0.110	0.974	0.197	0.953	0.143	0.966	0.106	0.975
(20,30)	0.185	0.956	0.117	0.972	0.083	0.980	0.152	0.964	0.105	0.975	0.082	0.980
(20,50)	0.175	0.959	0.110	0.974	0.072	0.982	0.144	0.966	0.099	0.976	0.069	0.983
(40,50)	0.154	0.963	0.094	0.977	0.064	0.984	0.126	0.970	0.084	0.980	0.063	0.984
(30,80)	0.113	0.973	0.069	0.983	0.061	0.985	0.100	0.976	0.069	0.983	0.059	0.985
(60,80)	0.094	0.977	0.058	0.986	0.052	0.987	0.083	0.980	0.058	0.986	0.052	0.987
$\phi = 0.8$												
(10,30)	0.238	0.944	0.178	0.958	0.128	0.970	0.209	0.951	0.151	0.964	0.112	0.973
(20,30)	0.204	0.952	0.142	0.966	0.104	0.975	0.177	0.958	0.141	0.967	0.100	0.976
(20,50)	0.182	0.957	0.111	0.973	0.072	0.982	0.149	0.965	0.099	0.976	0.070	0.983
(40,50)	0.169	0.960	0.105	0.975	0.071	0.983	0.140	0.967	0.097	0.977	0.069	0.983
(30,80)	0.134	0.968	0.080	0.980	0.062	0.985	0.114	0.973	0.076	0.981	0.062	0.985
(60,80)	0.113	0.973	0.068	0.983	0.054	0.987	0.096	0.977	0.064	0.984	0.053	0.987

5. Real data applications

To demonstrate the practical applicability and flexibility of the proposed methodology, this section analyzes two real-world datasets from distinct scientific fields. The first application arises from environmental toxicology and examines the relationship between airborne exposure and urinary metabolite concentrations as indicators of human exposure to hazardous contaminants. The second application is drawn from economic geology and focuses on diamond size data from a major mining area in southwest Africa, where accurate characterization is essential for resource evaluation and economic assessment. Both datasets are presented in Table 11.

Now, we present the following brief discussion of the datasets that were examined:

- **Environmental Toxicology:** Airborne exposure to environmental and occupational contaminants is a significant public health concern because inhalation allows chemicals to rapidly enter the human body. Many airborne pollutants, including volatile organic compounds, polycyclic aromatic hydrocarbons, and industrial chemicals, are metabolized and excreted as urinary metabolites that can be used as biomarkers of exposure. Urinary biomonitoring is widely used because it is non-invasive and reflects recent internal exposure to toxic substances; see Vahter et al. [28]. However, urinary metabolite concentrations are also influenced by factors such as age, sex, metabolic rate, hydration status, and renal function. Motivated by this importance, we examine in this part the variations in airborne exposure (VIE) and the concentration of urinary metabolites. This dataset was first provided by Kumagai and Matsunaga [29] and later rediscussed by Peter et al. [30].
- **Economic Geology:** Africa hosts some of the world's most significant diamond deposits, including extensive kimberlite, alluvial, and marine resources that contribute substantially to regional economic development and global diamond supply. The diamond industry in this region plays an important role in employment generation, export revenue, infrastructure development, and technological advancement within the mining sector. Furthermore, scientific investigation of diamond deposits in Africa (DSA) yields valuable insights into regional geology, sedimentary processes, and resource management strategies that support sustainable exploration and mining practices. Accurate diamond size characterization is critical for reliable grade estimation, revenue forecasting, and economic assessment, given the strong influence of stone size on diamond value. In this application, a dataset consists of diamond sizes from a large mining area in southwest Africa; see Mohammed et al. [18] and Maurya and Goyal [31].

Table 11. Two datasets from environmental toxicology and economic geology.

VIE Data										
1.5	1.7	2.1	2.2	2.4	2.5	2.6	3.8	3.8	4.2	4.3
5.6	6	7	7.5	9.3	9.9	10.2	10.6	12.3	12.9	13.7
14.1	17.8	27.6	31	42	45.6	51.9	91.3	131.8		
DSA Data										
1	1	1.5	2	2	2	2	2.5	3	3	4.5
5	7	7	7.5	9	16.5	20.5	28	39	40.5	69.5
137	257.5	358								

Before constructing the proposed inferential procedures, the appropriateness of the INH distribution for modeling the VIE and DSA datasets was first investigated. For this purpose, the MLEs of the parameters σ and μ, together with their corresponding standard errors (SEs) and 95% ACIs, were obtained and reported in Table 12. The associated interval widths (IWs) are also included for comparison. Using the fitted values $\hat{\sigma}$ and $\hat{\mu}$ obtained from the complete VIE and DSA datasets, the goodness-of-fit of the INH model was further assessed through the Kolmogorov–Smirnov ($\mathcal{KS}$) test. The resulting $\mathcal{KS}$ statistic and its corresponding $\mathcal{P}$-value are presented in Table 12. Since the computed $\mathcal{P}$-value is substantially larger than the nominal significance level ($\alpha = 5\%$), the null hypothesis cannot be rejected. This finding indicates that the INH distribution provides an adequate fit to the observed VIE and DSA datasets.

Table 12. Fit results for the INH model from the VIE and DSA datasets.

Par.	MLE(SE)	95% ACI			$\mathcal{KS}$($\mathcal{P}$-value)
		Low.	Upp.	IW	
VIE Data					
σ	1.0976(0.5918)	0.0062	2.2576	2.2514	0.0957(0.9391)
μ	4.5268(3.8622)	-	12.096	12.096	
DSA Data					
σ	0.6075(0.2807)	0.0574	1.1576	2.2514	0.1339(0.7614)
μ	9.0211(8.6242)	-	25.925	25.925	

To provide more fit investigations for the INH model framework, Figure 2 presents the total-time-on-test (TTT) transform plots and violin/boxplots for the VIE and DSA datasets. The TTT plots are useful for identifying the underlying hazard rate behavior, while the violin and boxplots provide insight into the distributional characteristics, spread, and potential outliers in the data. For the VIE and DSA datasets, the estimated TTT curves suggest upside-down then bathtub-shaped and decreasing failure rate behaviors, respectively. The violin/boxplots reveal that both datasets are positively skewed, with the DSA data displaying substantially larger variability and more extreme outliers compared with the VIE data. Overall, these graphical analyses confirm the presence of heterogeneous distributional patterns and support the suitability of flexible statistical modeling for both applications.

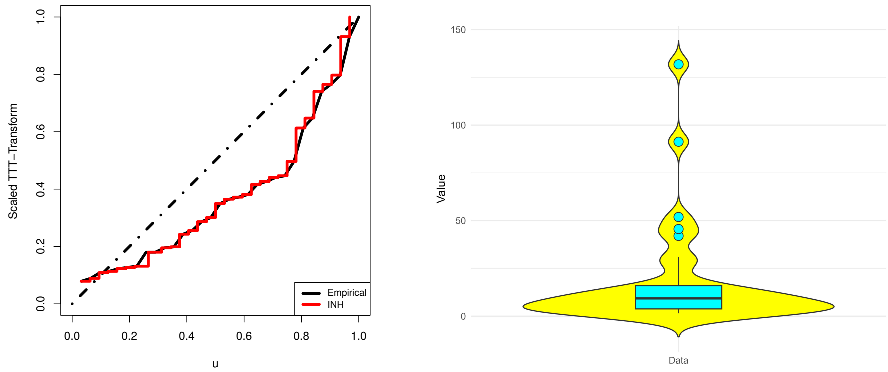

(a) VIE data

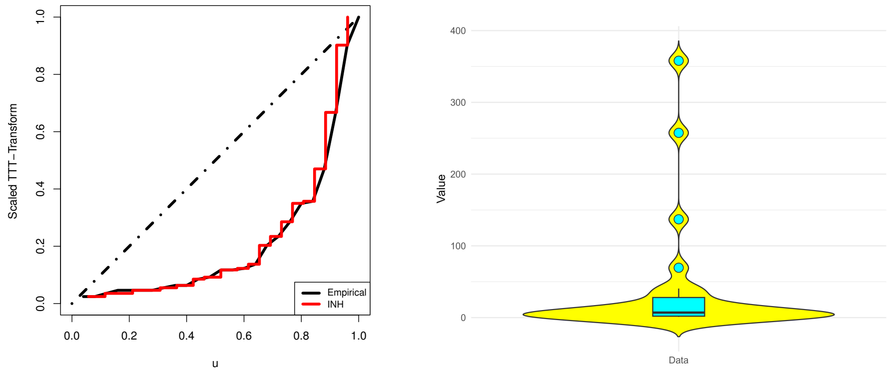

(b) DSA data

(i) TTT (ii) Violin/Boxplot

Figure 2. The TTT and violin diagrams of the INH model from VIE and DSA datasets.

To further assess the adequacy of the fitted model, several graphical diagnostic tools were employed. In particular, Figures 3 and 4 present a detailed visual evaluation of the INH model through four complementary plots: (a) contour plots of the log-likelihood function, (b) empirical and fitted reliability curves, (c) empirical versus fitted probability–probability (PP) plots, and (d) empirical versus fitted quantile–quantile (QQ) plots.

It is worth noticing here that the empirical cumulative probabilities used in the PP plots were calculated according to the Weibull plotting-position formula,

$$\widehat{F}(x_{(i)}) = \frac{i}{n+1}, \qquad i = 1, \ldots, n,$$

where $x_{(i)}$ denotes the ith ordered observation.

Panel (a) of Figures 3 and 4 provide clear empirical evidence regarding the existence and uniqueness of the MLEs $\hat{\sigma}$ and $\hat{\mu}$ obtained from the VIE and DSA datasets. Accordingly, the estimated values of $\hat{\sigma}$ and $\hat{\mu}$ reported in Table 12 are adopted as initial values in the subsequent computational algorithms to improve numerical stability and computational efficiency. Moreover, the graphical patterns displayed in panels (b)–(d) of Figures 3 and 4 indicate a close agreement between the empirical observations and the fitted INH model. These diagnostic plots further confirm the capability of the INH distribution to adequately describe the underlying behavior of the VIE and DSA datasets, which is consistent with the inferential results summarized in Table 12.

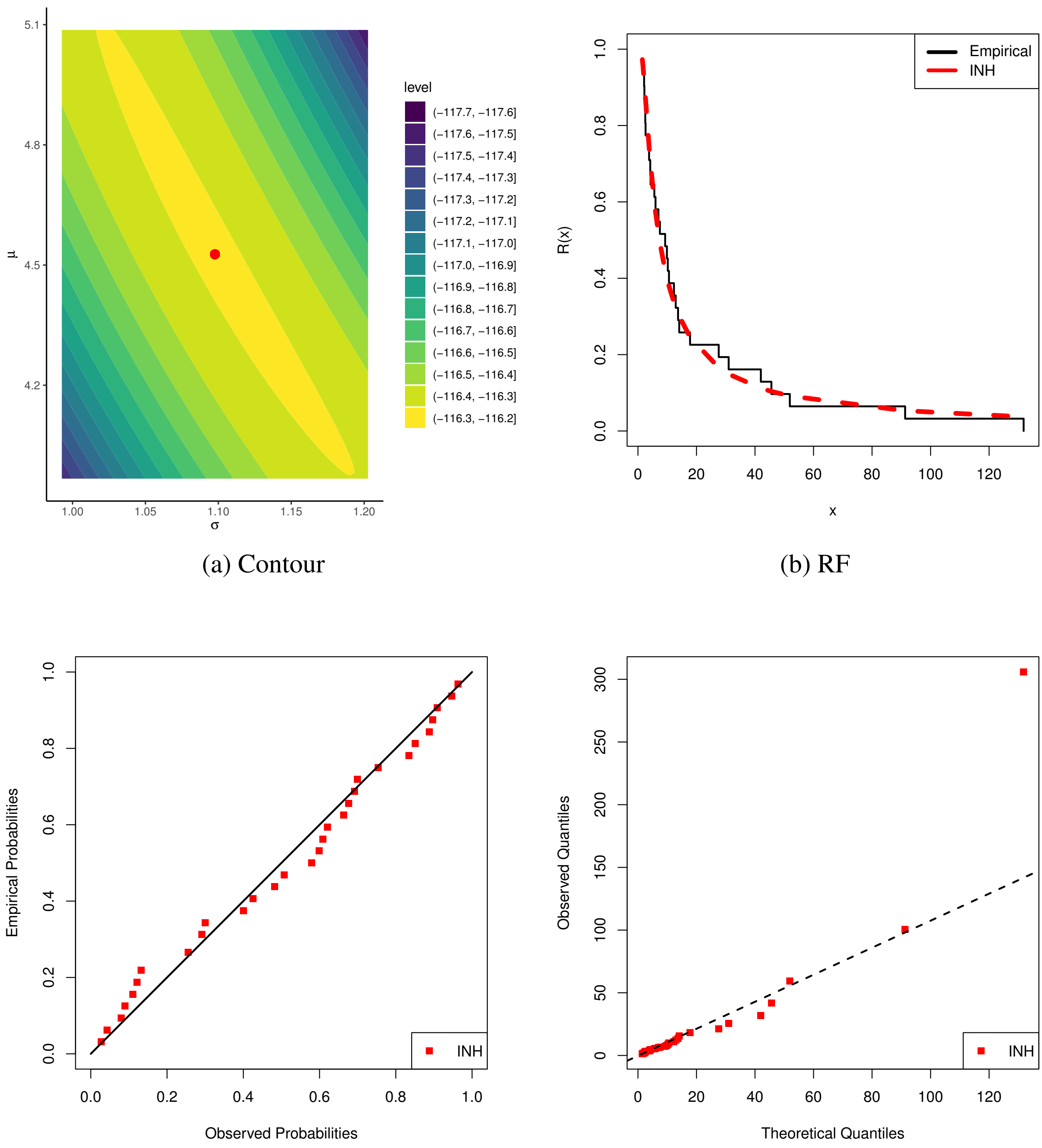

(a) Contour (b) RF

(c) PP (d) QQ

Figure 3. Fitting diagrams for the estimated INH model from VIE data.

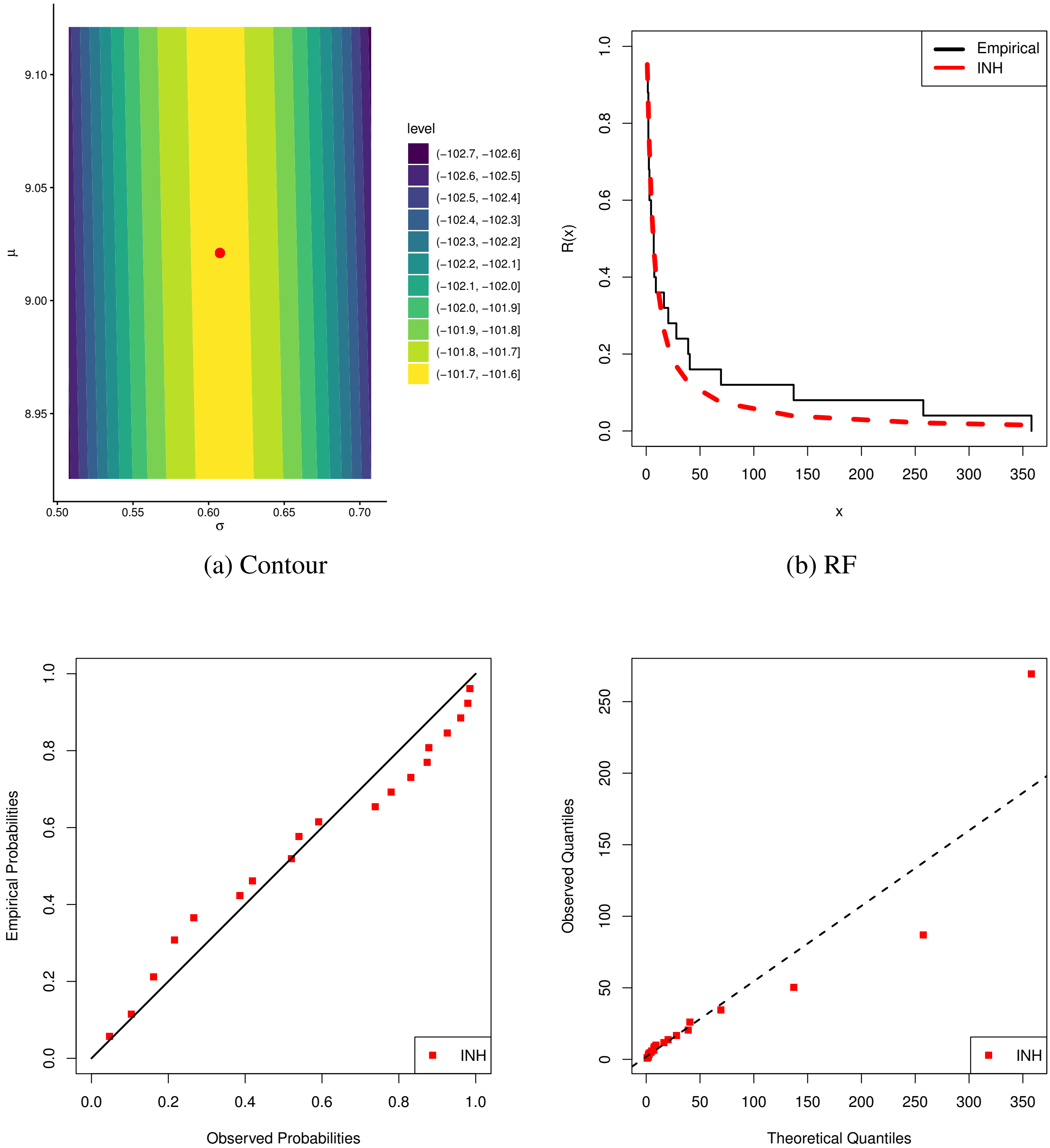

(a) Contour (b) RF

(c) PP (d) QQ

Figure 4. Fitting diagrams for the estimated INH model from DSA data.

Before presenting the inferential results developed in the previous sections, we first examine the adequacy of the baseline INH lifetime model by comparing its fitting performance with several well-established lifetime distributions from the reliability literature. To this end, the complete VIE and DSA datasets were analyzed using the INH distribution together with twelve competing models (see Table 13), covering a broad spectrum of lifetime behaviors and hazard-rate characteristics. The comparative assessment was carried out using four widely adopted information-based criteria, namely, (i) Akaike (A), (ii) consistent Akaike (CA), (iii) Bayesian (B), and (iv) Hannan-Quinn (HQ). Using the AdequacyModel package (by Marinho et al. [32]), the MLEs (together with their SEs) of ξ, σ, and μ were obtained; see Table 2. The same table also reports the values of the model selection criteria for all competing distributions. According to the adopted information criteria, where smaller values indicate a superior fit, the INH distribution consistently provides the best overall performance for both the VIE and DSA datasets. These results demonstrate that the INH distribution offers a flexible and reliable representation of the considered VIE and DSA lifetime datasets, thereby providing a sound foundation for the proposed censoring framework and the subsequent inferential procedures.

Table 13. Several competitors of the INH distribution.

Model	Symbol	Author(s)
Inverted generalized gamma	IGG(ξ,σ,μ)	Alotaibi et al. [33]
Generalized inverse Gompertz	GIG(ξ,σ,μ)	Elshahhat et al. [34]
Generalized inverse Weibull	GIW(ξ,σ,μ)	De Gusmao et al. [35]
Inverse log-logistic	ILL(ξ,σ,μ)	Chiodo et al. [36]
Inverted exponentiated Weibull	IEW(ξ,σ,μ)	Lee et al. [37]
Inverted Dagum	IDag(ξ,σ,μ)	Osi et al. [38]
Alpha power inverse Weibull	APIW(ξ,σ,μ)	Basheer [39]
Inverted exponentiated Pareto	IEP(σ,μ)	Abouammoh and Alshingiti [40]
Exponentiated inverted exponential	EIE(σ,μ)	Fatima and Ahmad [41]
Inverted Kumaraswamy	IK(σ,μ)	Abd AL-Fattah et al. [42]
Inverted Lomax	ILo(σ,μ)	Kleiber and Kotz [43]
Inverted Weibull	IW(σ,μ)	Khan et al. [44]

Table 14. Fitting summary of the INH and others from the VIE and DSA datasets.

Model	ξ		σ		μ		A	CA	B	HQ
	Est.	SE	Est.	SE	Est.	SE				
VIE Data										
INH	-	-	1.1009	0.5927	4.5052	3.8338	236.58	237.01	239.45	237.51
IGG	0.8656	0.8010	1.3193	2.0066	7.6439	18.432	238.54	239.43	242.84	239.94
GIG	0.9538	0.3088	4.5571	2.3386	0.5549	1.6022	238.43	239.32	242.73	239.83
GIW	1.0257	0.1455	2.5682	536.46	2.0553	440.33	238.58	239.47	242.88	239.98
ILL	7.6598	5.0189	1.1216	0.1641	0.8802	0.6385	239.03	239.92	243.33	240.43
IEW	0.8757	1.0750	1.3266	2.9030	5.3066	1.3336	238.57	239.46	242.88	239.98
IDag	1.0761	0.2129	5.8228	11.293	1.1464	2.5892	239.11	239.99	243.41	240.51
APIW	1.9431	3.5978	1.0917	0.2206	4.9649	1.9936	238.45	239.34	242.76	239.86
IEP	-	-	1.1785	0.2839	6.7464	1.5127	237.05	237.48	239.92	237.98
EIE	-	-	0.1192	0.0984	2.1465	1.6454	246.84	247.27	249.71	247.77
IK	-	-	1.1279	0.1869	7.6088	2.7847	237.01	237.44	239.88	237.95
IL	-	-	21.238	32.261	0.2560	0.4054	236.81	237.24	239.68	237.75
IW	-	-	1.0260	0.1455	5.4118	1.3719	236.58	237.10	239.55	237.58
DSA Data										
INH	-	-	0.6064	0.2804	9.0572	8.6745	205.26	205.80	207.67	205.93
IGG	2.6688	2.6481	0.1954	0.2312	1.1701	0.4404	206.24	207.39	209.90	207.26
GIG	0.5579	0.1714	1.6273	1.0515	1.1612	1.1394	206.09	207.24	209.75	207.11
GIW	0.7826	0.1282	1.2695	28.182	2.5069	43.555	207.71	208.85	211.36	208.72
ILL	5.8949	3.1383	0.8246	0.1374	0.5121	0.4117	208.72	209.86	212.38	209.73
IEW	2.4736	3.0345	0.2112	0.3097	2.1814	1.3224	206.21	207.35	209.86	207.22
IDag	0.8215	0.1642	7.7651	18.127	0.3776	1.2873	208.44	209.58	212.10	209.46
APIW	0.6759	1.2017	0.7521	0.1924	3.2165	1.0927	207.66	208.80	211.32	208.67
IEP	-	-	0.7433	0.1832	3.7213	1.0480	206.58	207.12	209.02	207.25
EIE	-	-	0.0136	0.0196	0.5553	0.7968	239.63	240.17	242.06	240.30
IK	-	-	0.8010	0.1674	3.3064	1.1318	206.85	207.40	209.29	207.53
IL	-	-	7.6591	20.912	0.5396	1.6610	208.06	208.61	210.50	208.74
IW	-	-	0.7827	0.1282	3.0219	0.6992	205.71	206.25	208.15	206.38

Using the VIE and DSA observations reported in Table 11, several APTIIC samples with random binomial removals, denoted by $\mathcal{S}[ij]$, $i = 1, 2$ and $j = 1, 2, \ldots, 4$, were generated under different combinations of the design parameters T, m, and ϕ; see Table 15.

Table 15. Artificial APTIIC samples with binomial removals from the VIE and DSA datasets.

VIE Samples											
Sample		$(\phi, m) = (0.3, 10)$ and $\{T(k), S_m\} = \{5(4), 6\}$									
$\mathcal{S}[11]$	i	1	2	3	4	5	6	7	8	9	10
	s_i	4	5	4	2	0	0	0	0	0	0
	x_i	1.5	2.1	3.8	4.2	7.5	9.3	10.6	13.7	27.6	42
		$(\phi, m) = (0.6, 10)$ and $\{T(k), S_m\} = \{3(2), 3\}$									
$\mathcal{S}[12]$	i	1	2	3	4	5	6	7	8	9	10
	s_i	15	3	0	0	0	0	0	0	0	0
	x_i	1.5	2.5	3.8	4.3	6	9.3	12.9	14.1	27.6	91.3
		$(\phi, m) = (0.3, 20)$ and $\{T(k), S_m\} = \{3(4), 3\}$									
$\mathcal{S}[13]$	i	1	2	3	4	5	6	7	8	9	10
	s_i	2	3	2	1	0	0	0	0	0	0
	x_i	1.5	2.2	2.5	2.6	3.8	4.3	5.6	6	7.5	9.9
	i	11	12	13	14	15	16	17	18	19	20
	s_i	0	0	0	0	0	0	0	0	0	0
	x_i	10.6	12.3	13.7	14.1	17.8	27.6	31	42	51.9	91.3
		$(\phi, m) = (0.6, 20)$ and $\{T(k), S_m\} = \{3(2), 1\}$									
$\mathcal{S}[14]$	i	1	2	3	4	5	6	7	8	9	10
	s_i	9	1	0	0	0	0	0	0	0	0
	x_i	1.5	2.4	3.8	4.2	5.6	6	7	7.5	9.9	10.2
	i	11	12	13	14	15	16	17	18	19	20
	s_i	0	0	0	0	0	0	0	0	0	0
	x_i	12.9	13.7	14.1	17.8	31	42	45.6	51.9	91.3	131.8
DSA Samples											
		$(\phi, m) = (0.3, 10)$ and $\{T(k), S_m\} = \{4(4), 4\}$									
$\mathcal{S}[21]$	i	1	2	3	4	5	6	7	8	9	10
	s_i	2	4	3	2	0	0	0	0	0	0
	x_i	1	2	2.5	3	5	7.5	16.5	39	137	257.5
		$(\phi, m) = (0.6, 10)$ and $\{T(k), S_m\} = \{2(2), 2\}$									
$\mathcal{S}[22]$	i	1	2	3	4	5	6	7	8	9	10
	s_i	11	2	0	0	0	0	0	0	0	0
	x_i	1	1.5	3	4.5	7	9	28	40.5	69.5	137
		$(\phi, m) = (0.3, 20)$ and $\{T(k), S_m\} = \{2(3), 2\}$									
$\mathcal{S}[23]$	i	1	2	3	4	5	6	7	8	9	10
	s_i	0	2	1	0	0	0	0	0	0	0
	x_i	1	1	1.5	2	2	2.5	3	4.5	5	7
	i	11	12	13	14	15	16	17	18	19	20
	s_i	0	0	0	0	0	0	0	0	0	0
	x_i	7.5	9	16.5	20.5	28	39	40.5	69.5	137	257.5
		$(\phi, m) = (0.6, 20)$ and $\{T(k), S_m\} = \{1(1), 1\}$									
$\mathcal{S}[24]$	i	1	2	3	4	5	6	7	8	9	10
	s_i	4	0	0	0	0	0	0	0	0	0
	x_i	1	1	2	2	2	2.5	3	3	4.5	5
	i	11	12	13	14	15	16	17	18	19	20
	s_i	0	0	0	0	0	0	0	0	0	0
	x_i	7	7	9	16.5	20.5	28	39	40.5	69.5	137

Under noninformative prior assumptions for σ, μ, and ϕ, improper gamma and beta prior distributions were adopted. The Bayesian computations were performed using $N = 50{,}000$ MCMC iterations, including the first 10,000 iterations discarded as burn-in samples, to obtain the Bayes point estimates and BCIs of σ, μ, $R(t)$, $h(t)$, and ϕ. For each generated sample listed in Table 15, the MLEs together with their SEs, as well as the corresponding 95% ACI and BCI estimates and their associated IWs, were calculated for σ, μ, $R(t)$ at $t = 5$, and ϕ; see Table 16.

Table 16. Estimates of σ, μ, $R(t)$, $h(t)$, and ϕ from the VIE and DSA datasets.

Sample	Par.	MLE		Bayes		ACI			BCI		
		Est.	SE	Est.	SE	Low.	Upp.	IW	Low.	Upp.	IW
VIE Samples											
$\mathcal{S}[11]$	σ	0.4254	0.0533	0.4221	0.0450	0.3209	0.5299	0.2091	0.3357	0.5097	0.1740
	μ	58.438	7.2459	58.436	0.1010	44.236	72.640	28.403	58.240	58.635	0.3947
	$R(t)$	0.8573	0.0539	0.8484	0.0500	0.7517	0.9629	0.2113	0.7399	0.9295	0.1896
	$h(t)$	0.0384	0.0076	0.0389	0.0065	0.0235	0.0534	0.0299	0.0260	0.0510	0.0250
	ϕ	0.2586	0.0575	0.2597	0.0699	0.1459	0.3713	0.2254	0.1566	0.3799	0.2234
$\mathcal{S}[12]$	σ	0.5423	0.1212	0.5389	0.0564	0.3048	0.7797	0.4749	0.4312	0.6510	0.2198
	μ	25.289	12.067	25.287	0.1005	1.6379	48.941	47.303	25.090	25.485	0.3947
	$R(t)$	0.8091	0.0655	0.8017	0.0524	0.6808	0.9374	0.2566	0.6909	0.8926	0.2017
	$h(t)$	0.0567	0.0139	0.0570	0.0071	0.0296	0.0839	0.0544	0.0423	0.0700	0.0278
	ϕ	0.6667	0.0907	0.6652	0.3758	0.4889	0.8445	0.3556	0.4801	0.8264	0.3464
$\mathcal{S}[13]$	σ	0.6483	0.3501	0.6438	0.0594	0.0038	1.3344	1.3306	0.5297	0.7608	0.2311
	μ	15.478	17.764	15.476	0.1003	0.0000	50.296	50.296	15.281	15.674	0.3928
	$R(t)$	0.7756	0.0735	0.7691	0.0477	0.6315	0.9197	0.2882	0.6707	0.8537	0.1830
	$h(t)$	0.0707	0.0312	0.0710	0.0066	0.0097	0.1318	0.1221	0.0576	0.0830	0.0254
	ϕ	0.2667	0.0807	0.2686	0.0853	0.1084	0.4249	0.3165	0.1299	0.4379	0.3081
$\mathcal{S}[14]$	σ	0.7255	0.2233	0.7211	0.0654	0.2877	1.1632	0.8755	0.5959	0.8506	0.2546
	μ	13.656	8.1113	13.654	0.1002	0.0000	29.554	29.554	13.459	13.851	0.3925
	$R(t)$	0.7980	0.0648	0.7918	0.0460	0.6710	0.9249	0.2539	0.6961	0.8731	0.1770
	$h(t)$	0.0699	0.0185	0.0702	0.0072	0.0336	0.1062	0.0725	0.0555	0.0834	0.0279
	ϕ	0.7692	0.1169	0.7648	0.1992	0.5402	0.9983	0.4581	0.5136	0.9409	0.4273
DSA Samples											
$\mathcal{S}[21]$	σ	0.2151	0.0278	0.2129	0.0242	0.1607	0.2695	0.1088	0.1660	0.2600	0.0940
	μ	677.28	11.8672	677.28	0.0505	654.02	700.54	46.519	677.18	677.38	0.1980
	$R(t)$	0.8473	0.0600	0.8366	0.0548	0.7297	0.9648	0.2351	0.7168	0.9250	0.2082
	$h(t)$	0.0222	0.0044	0.0224	0.0037	0.0136	0.0308	0.0172	0.0150	0.0294	0.0144
	ϕ	0.2558	0.0665	0.2570	0.0788	0.1254	0.3862	0.2608	0.1393	0.3963	0.2570
$\mathcal{S}[22]$	σ	0.3337	0.0474	0.3315	0.0335	0.2408	0.4265	0.1857	0.2678	0.3981	0.1303
	μ	81.375	12.384	81.375	0.0502	57.104	105.65	48.544	81.277	81.474	0.1965
	$R(t)$	0.7956	0.0686	0.7886	0.0514	0.6612	0.9300	0.2687	0.6816	0.8787	0.1971
	$h(t)$	0.0418	0.0068	0.0420	0.0047	0.0284	0.0552	0.0268	0.0322	0.0505	0.0183
	ϕ	0.6842	0.1066	0.6817	0.1320	0.4752	0.8932	0.4180	0.4621	0.8634	0.4013
$\mathcal{S}[23]$	σ	0.3714	0.0575	0.3688	0.0340	0.2587	0.4840	0.2253	0.3034	0.4357	0.1323
	μ	37.322	10.401	37.321	0.0502	16.936	57.707	40.771	37.223	37.420	0.1965
	$R(t)$	0.7019	0.0664	0.6962	0.0483	0.5718	0.8320	0.2602	0.5981	0.7848	0.1866
	$h(t)$	0.0615	0.0081	0.0616	0.0039	0.0455	0.0774	0.0319	0.0534	0.0687	0.0153
	ϕ	0.2308	0.1169	0.2352	0.1293	0.0017	0.4598	0.4581	0.0590	0.4864	0.4274
$\mathcal{S}[24]$	σ	0.6105	0.1861	0.6078	0.0420	0.2457	0.9752	0.7295	0.5252	0.6895	0.1642
	μ	9.5935	5.8589	9.5926	0.0503	0.0000	21.077	21.077	9.4944	9.6918	0.1975
	$R(t)$	0.6027	0.0795	0.5998	0.0345	0.4468	0.7585	0.3117	0.5299	0.6647	0.1348
	$h(t)$	0.1018	0.0218	0.1018	0.0030	0.0589	0.1446	0.0856	0.0956	0.1075	0.0118
	ϕ	0.8000	0.1789	0.7877	0.2492	0.4494	1.1506	0.7012	0.3905	0.9908	0.6003

Table 17. Statistics of σ, μ, $R(t)$, $h(t)$, and ϕ from the VIE and DSA datasets.

Sample	Par.	Mean	Mode	$\mathbb{Q}_1$	$\mathbb{Q}_2$	$\mathbb{Q}_3$	St.D	Skew.
VIE Samples								
$\mathcal{S}[11]$	σ	0.4221	0.4434	0.3911	0.4216	0.4527	0.0449	0.0537
	μ	58.436	58.400	58.368	58.436	58.505	0.1010	0.0220
	$R(t)$	0.8484	0.8756	0.8175	0.8532	0.8845	0.0492	-0.5509
	$h(t)$	0.0389	0.0358	0.0344	0.0390	0.0434	0.0065	-0.1157
	ϕ	0.2597	0.0779	0.2196	0.2569	0.2970	0.0571	0.2957
$\mathcal{S}[12]$	σ	0.5389	0.5246	0.5004	0.5376	0.5767	0.0563	0.0981
	μ	25.287	25.183	25.218	25.287	25.356	0.1004	0.0233
	$R(t)$	0.8017	0.7916	0.7685	0.8047	0.8389	0.0519	-0.3907
	$h(t)$	0.0570	0.0572	0.0523	0.0574	0.0620	0.0071	-0.2511
	ϕ	0.6652	0.2626	0.6071	0.6695	0.7279	0.0887	-0.2674
$\mathcal{S}[13]$	σ	0.6438	0.6416	0.6033	0.6434	0.6848	0.0592	0.0205
	μ	15.476	15.345	15.408	15.476	15.544	0.1003	0.0193
	$R(t)$	0.7691	0.7679	0.7386	0.7717	0.8032	0.0472	-0.3334
	$h(t)$	0.0710	0.0720	0.0666	0.0713	0.0756	0.0066	-0.1976
	ϕ	0.2686	0.0490	0.2117	0.2634	0.3203	0.0793	0.3754
$\mathcal{S}[14]$	σ	0.7211	0.6786	0.6765	0.7206	0.7661	0.0652	0.0328
	μ	13.654	13.543	13.586	13.654	13.722	0.1002	0.0202
	$R(t)$	0.7918	0.7616	0.7622	0.7946	0.8247	0.0456	-0.3556
	$h(t)$	0.0702	0.0640	0.0653	0.0705	0.0753	0.0072	-0.1822
	ϕ	0.7648	0.2551	0.6943	0.7784	0.8490	0.1119	-0.6185
DSA Samples								
$\mathcal{S}[21]$	σ	0.2129	0.2083	0.1964	0.2128	0.2293	0.0241	0.0274
	μ	677.28	677.27	677.25	677.28	677.32	0.0505	0.0076
	$R(t)$	0.8366	0.8322	0.8033	0.8421	0.8759	0.0538	-0.5899
	$h(t)$	0.0224	0.0232	0.0199	0.0225	0.0251	0.0037	-0.1237
	ϕ	0.2570	0.0469	0.2102	0.2531	0.3002	0.0660	0.3100
$\mathcal{S}[22]$	σ	0.3315	0.3102	0.3087	0.3311	0.3544	0.0335	0.0571
	μ	81.375	81.319	81.341	81.375	81.409	0.0502	0.0221
	$R(t)$	0.7886	0.7583	0.7557	0.7918	0.8253	0.0509	-0.3719
	$h(t)$	0.0420	0.0379	0.0388	0.0422	0.0453	0.0047	-0.2249
	ϕ	0.6817	0.1360	0.6133	0.6883	0.7568	0.1036	-0.3446
$\mathcal{S}[23]$	σ	0.3688	0.3479	0.3456	0.3686	0.3921	0.0339	0.0196
	μ	37.321	37.265	37.287	37.321	37.355	0.0502	0.0223
	$R(t)$	0.6962	0.6676	0.6646	0.6981	0.7303	0.0480	-0.2315
	$h(t)$	0.0616	0.0583	0.0590	0.0618	0.0644	0.0039	-0.2543
	ϕ	0.2352	0.0078	0.1510	0.2216	0.3057	0.1119	0.6185
$\mathcal{S}[24]$	σ	0.6078	0.5826	0.5794	0.6078	0.6362	0.0419	0.0082
	μ	9.5926	9.5605	9.5586	9.5924	9.6266	0.0503	0.0298
	$R(t)$	0.5998	0.5812	0.5768	0.6005	0.6233	0.0344	-0.1134
	$h(t)$	0.1018	0.1018	0.0999	0.1020	0.1040	0.0030	-0.2165
	ϕ	0.7877	0.0856	0.6917	0.8258	0.9188	0.1639	-0.9671

The numerical findings reported in Table 16 reveal that the Bayesian estimates of σ, μ, $R(t)$, $h(t)$, and ϕ exhibit better performance than the corresponding likelihood-based estimates, as reflected by their smaller SE values. Moreover, the estimated BCIs appear to be more efficient than the corresponding ACIs due to their relatively shorter IWs.

To investigate the existence and uniqueness of the MLEs corresponding to the parameters σ and μ of the INH(σ, μ) model, Figure 5 depicts the contour surfaces of the log-likelihood function under several combinations of (σ, μ). The displayed contours reveal a well-defined global maximum, confirming both the existence and uniqueness of the obtained estimators $\hat{\sigma}$ and $\hat{\mu}$. These graphical observations are in agreement with the numerical estimates reported in Table 16.

Therefore, the resulting MLEs are utilized as starting values in the Bayesian computational procedure for each replicate in $\mathcal{S}[ij]$, $i = 1, 2$, $j = 1, 2, 3, 4$. To assess the convergence properties of the MCMC implementation, Figure 6 illustrates the trace plots and posterior density plots associated with the remaining 40,000 generated observations of σ, μ, $R(t)$, $h(t)$, and ϕ obtained from the samples $\mathcal{S}[i1]$, $i = 1, 2$, for illustrative purposes. The trace plots demonstrate stable mixing behavior without noticeable trends, while the posterior density plots indicate well-behaved stationary distributions. These diagnostics suggest satisfactory convergence of the MH sampling scheme presented in Section 3, supporting the reliability of the posterior inference for the INH model parameters and the related reliability measures.

Furthermore, the posterior densities of σ, μ, and $h(t)$ appear nearly symmetric, whereas the posterior distribution of $R(t)$ and ϕ exhibits a moderate left- and right-skewed patterns, respectively. To complement the graphical analysis, Table 17 provides several descriptive summaries for the generated MCMC samples of σ, μ, $R(t)$, $h(t)$, and ϕ, including the posterior mean, mode, quartiles $(\mathbb{Q}_1, \mathbb{Q}_2, \mathbb{Q}_3)$, standard deviation, and skewness coefficient. The numerical characteristics reported in Table 17 are consistent with the graphical behavior observed in Figure 6, confirming the adequacy and stability of the posterior estimates.

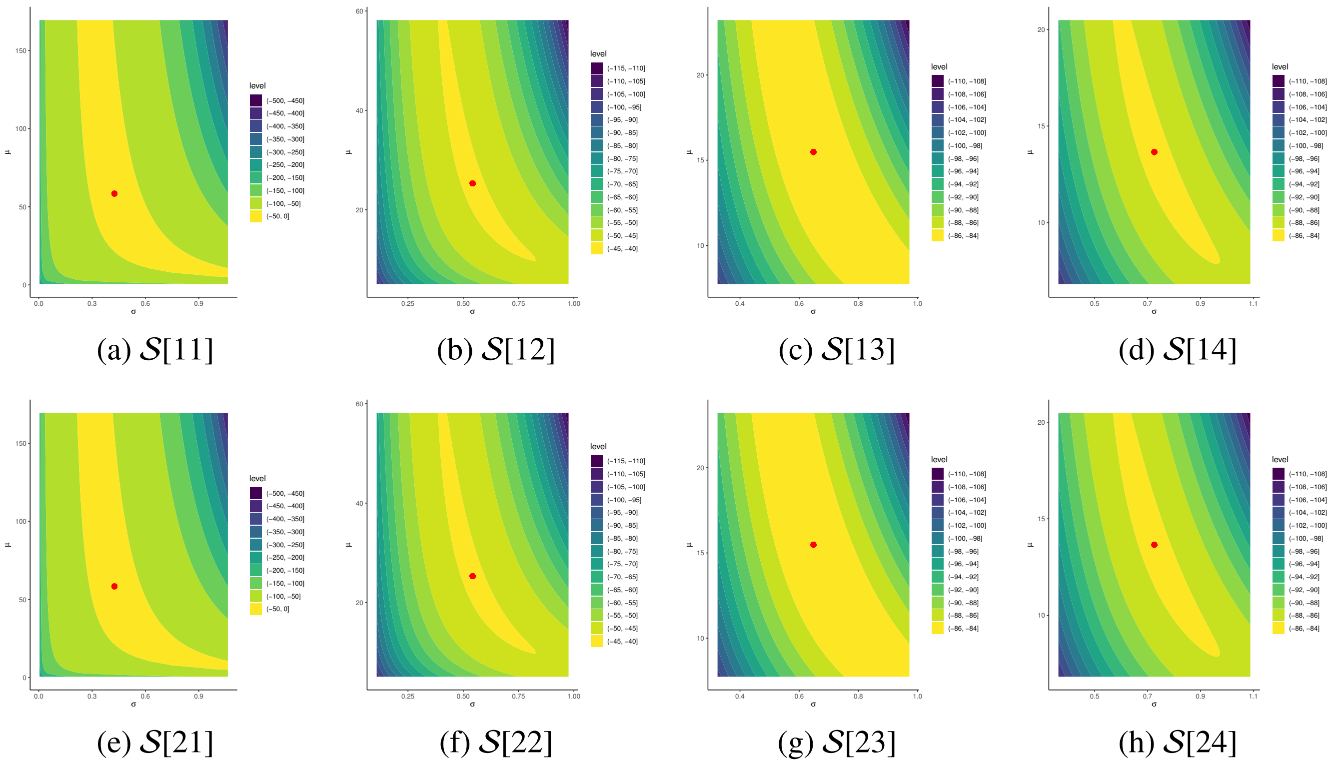

(a) $\mathcal{S}[11]$ (b) $\mathcal{S}[12]$ (c) $\mathcal{S}[13]$ (d) $\mathcal{S}[14]$

(e) $\mathcal{S}[21]$ (f) $\mathcal{S}[22]$ (g) $\mathcal{S}[23]$ (h) $\mathcal{S}[24]$

Figure 5. Contours of σ and μ from VIE data.

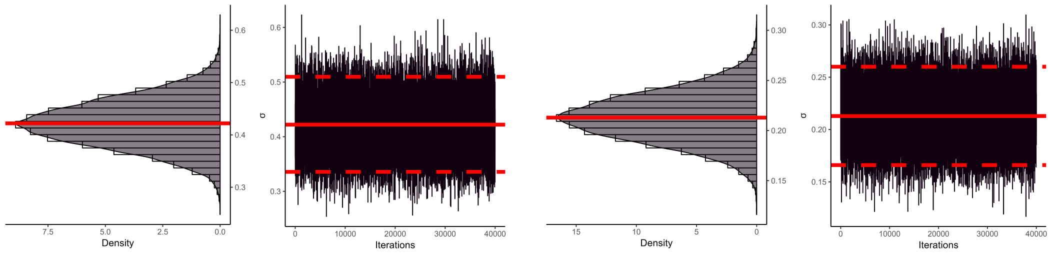

(a) σ

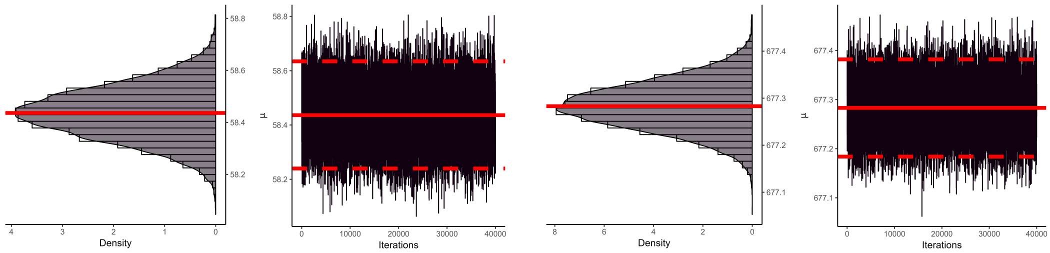

(b) μ

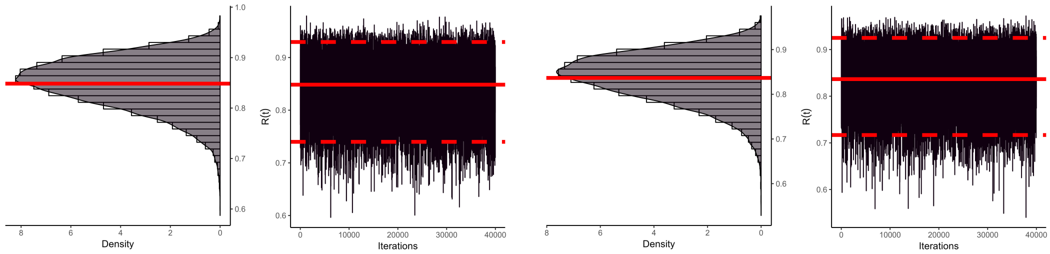

(c) $R(t)$

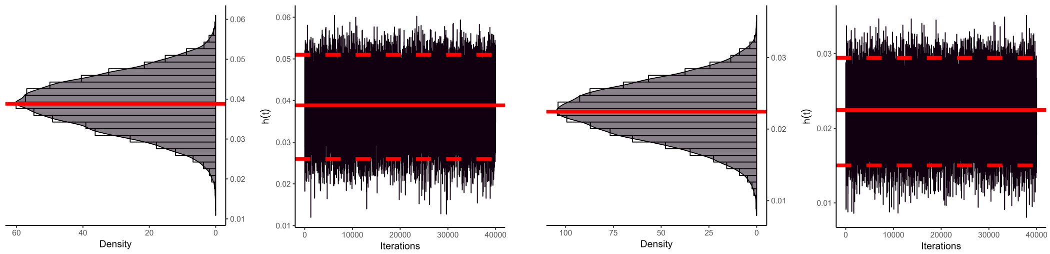

(d) $h(t)$

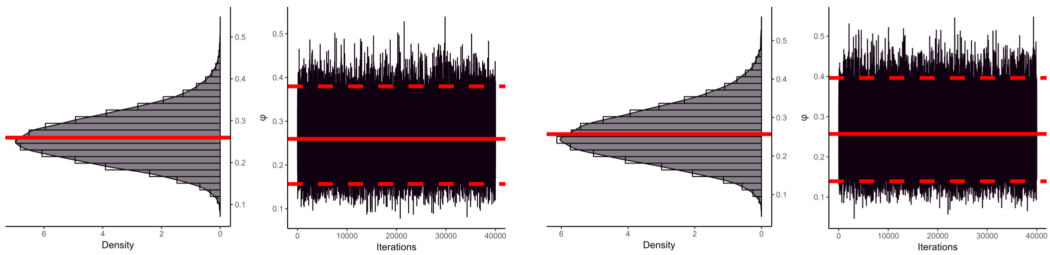

(e) ϕ

(i) VIE data (ii) DSA data

Figure 6. Convergence MCMC plots of σ, μ, $R(t)$, $h(t)$, and ϕ from VIE data.

6. Concluding remarks

This study introduced an inferential framework for the inverted Nadarajah–Haghighi distribution under an adaptive progressive Type-II censoring scheme with binomial removals. The proposed approach was motivated by the need to incorporate realistic removal mechanisms in life-testing experiments, where the number of withdrawn units is often governed by random operational factors. From the classical perspective, maximum likelihood estimation was developed for the model parameters and the binomial removal parameter, and approximate confidence intervals were constructed using the observed Fisher information matrix. In addition, the invariance property of maximum likelihood estimation was utilized to obtain the estimators of the reliability function and hazard rate function. From the Bayesian viewpoint, posterior inference was carried out under independent gamma priors for the model parameters and a beta prior for the binomial parameter. Due to the complexity of the posterior distributions, Markov chain Monte Carlo methods were employed to generate posterior samples, from which Bayes estimates and credible intervals were obtained for both the model parameters and the associated reliability measures. The performance of the proposed estimation procedures was examined through an extensive simulation study, which demonstrated their effectiveness in terms of accuracy and stability across different parameter settings and censoring scenarios. Furthermore, the applicability of the proposed methodology was illustrated using real datasets, where the model showed strong capability in capturing the underlying failure behavior and providing reliable estimates of key reliability measures. Overall, the proposed framework offers a flexible and robust tool for statistical inference in reliability analysis under complex censoring schemes. It is expected that this work will provide a useful foundation for future studies involving more general censoring mechanisms, alternative loss functions, and extended lifetime models.

The proposed inferential framework also provides several directions for future research. One possible extension is the development of analogous estimation procedures for competing risks models under adaptive progressive censoring with random removals, where multiple failure mechanisms are observed simultaneously. Another promising direction is the incorporation of the proposed methodology into accelerated life-testing frameworks, such as constant-stress or step-stress accelerated life tests, to facilitate efficient reliability assessment for highly reliable products under complex censoring schemes. Furthermore, the maximum product of spacings method may be explored as an alternative to the maximum likelihood method for parameter estimation, particularly in situations where it offers improved numerical stability or estimation performance. Future studies may also investigate Bayesian inference based on the maximum product of spacings criterion as an alternative to the conventional likelihood-based Bayesian approach. These extensions would further broaden the applicability and flexibility of the proposed framework in modern reliability and survival analysis.

Author contributions

Conceptualization: Refah Alotaibi and Mazen Nassar; Methodology: Refah Alotaibi and Mazen Nassar; Investigation: Mazen Nassar and Ahmed Elshahhat; Funding Acquisition: Refah Alotaibi; Formal Analysis: Mazen Nassar and Ahmed Elshahhat; Software / Coding: Ahmed Elshahhat; Visualization: Ahmed Elshahhat; Writing – Review & Editing: Refah Alotaibi, Mazen Nassar, and Ahmed Elshahhat.

Use of Generative-AI tools declaration

The authors declare that they have not used Artificial Intelligence (AI) tools in the creation of this article.

Acknowledgments

This research was funded by Princess Nourah bint Abdulrahman University Researchers Supporting Project number (PNURSP2026R50), Princess Nourah bint Abdulrahman University, Riyadh, Saudi Arabia.

Conflicts of interest

The authors declare no conflict of interest.

References

1. N. Balakrishnan, Progressive censoring methodology: an appraisal, *Test*, **16** (2007), 211–259. https://doi.org/10.1007/s11749-007-0061-y
2. E. S. Brito, P. H. Ferreira, V. L. Tomazella, D. S. Martins Neto, R. S. Ehlers, Inference methods for the Very Flexible Weibull distribution based on progressive type-II censoring, *Commun. Stat.-Simul. Comput.*, **53** (2024), 5342–5366. https://doi.org/10.1080/03610918.2023.2180646
3. E. H. Khalifa, D. A. Ramadan, H. N. Alqifari, B. S. El-Desouky, Bayesian Inference for Inverse Power Exponentiated Pareto Distribution Using Progressive Type-II Censoring with Application to Flood-Level Data Analysis, *Symmetry*, **16** (2024), 309. https://doi.org/10.3390/sym16030309
4. M. M. Hasaballah, Y. A. Tashkandy, O. S. Balogun, M. E. Bakr, Reliability analysis for two populations Nadarajah-Haghighi distribution under Joint progressive type-II censoring, *AIMS Math.*, **9** (2024), 10333–10352. https://doi.org/10.3934/math.2024505
5. H. K. T. Ng, D. Kundu, P. S. Chan, Statistical analysis of exponential lifetimes under an adaptive Type-II progressive censoring scheme, *Nav. Res. Log.*, **56** (2009), 687–698. https://doi.org/10.1002/nav.20371
6. D. Kundu, A. Joarder, Analysis of Type-II progressively hybrid censored data, *Comput. Stat. Data Anal.*, **50** (2006), 2509–2528. https://doi.org/10.1016/j.csda.2005.05.002
7. M. Nassar, O. E. Abo-Kasem, Estimation of the inverse Weibull parameters under adaptive type-II progressive hybrid censoring scheme, *J. Comput. Appl. Math.*, **315** (2017), 228–239. https://doi.org/10.1016/j.cam.2016.11.012
8. H. Panahi, N. Moradi, Estimation of the inverted exponentiated Rayleigh distribution based on adaptive Type II progressive hybrid censored sample, *J. Comput. Appl. Math.*, **364** (2020), 112345. https://doi.org/10.1016/j.cam.2019.112345
9. A. Elshahhat, M. Nassar, Bayesian survival analysis for adaptive Type-II progressive hybrid censored Hjorth data, *Computation. Stat.*, **36** (2021), 1965–1990. https://doi.org/10.1007/s00180-021-01065-8

10. S. Dutta, S. Dey, S. Kayal, Bayesian survival analysis of logistic exponential distribution for adaptive progressive Type-II censored data, *Computation. Stat.*, **39** (2024), 2109–2155. https://doi.org/10.1007/s00180-023-01376-y
11. A. Alrumayh, W. Weera, H. A. Khogeer, E. M. Almetwally, Optimal analysis of adaptive type-II progressive censored for new unit-lindley model, *J. King Saud Univ. Sci.*, **35** (2023), 102462. https://doi.org/10.1016/j.jksus.2022.102462
12. R. Kumari, F. Sultana, Y. M. Tripathi, R. K. Sinha, Parametric inference for inverted exponentiated family with jointly adaptive progressive type-II censoring, *Life Cycle Reliability and Safety Engineering*, **14** (2025), 37–56. https://doi.org/10.1007/s41872-024-00281-7
13. S. Nadarajah, F. Haghighi, An extension of the exponential distribution, *Statistics*, **45** (2011), 543–558. https://doi.org/10.1080/02331881003678678
14. M. H. Tahir, G. M. Cordeiro, S. Ali, S. Dey, A. Manzoor, The inverted Nadarajah–Haghighi distribution: estimation methods and applications, *J. Stat. Comput. Sim.*, **88** (2018), 2775–2798. https://doi.org/10.1080/00949655.2018.1487441
15. A. Elshahhat, M. K. Rastogi, Estimation of parameters of life for an inverted Nadarajah–Haghighi distribution from Type-II progressively censored samples, *J. Indian Soc. Prob. Stat.*, **22** (2021), 113–154. https://doi.org/10.1007/s41096-021-00097-z
16. O. E. Abo-Kasem, E. M. Almetwally, W. S. Abu El Azm, Inferential survival analysis for inverted NH distribution under adaptive progressive hybrid censoring with application of transformer insulation, *Annals of Data Science*, **10** (2023), 1237–1284. https://doi.org/10.1007/s40745-022-00409-5
17. T. A. Abushal, A. M. AL-Zaydi, Statistical inference of inverted Nadarajah–Haghighi distribution under type-II generalized hybrid censoring competing risks data, *J. Eng. Math.*, **144** (2024), 24. https://doi.org/10.1007/s10665-023-10331-1
18. H. S. Mohammed, O. E. Abo-Kasem, A. Elshahhat, Optimum Progressive Data Analysis and Bayesian Inference for Unified Progressive Hybrid INH Censoring with Applications to Diamonds and Gold, *Axioms*, **14** (2025), 559. https://doi.org/10.3390/axioms14080559
19. O. A. Alqasem, A. Elshahhat, M. E. Abd Elwahab, M. Nassar, Evaluation of two inverted Nadarajah–Haghighi production lines via joint progressive type-II censoring with two physical applications, *AIP Advances*, **15** (2025). https://doi.org/10.1063/5.0249890
20. A. Elshahhat, M. Nassar, Analysis of adaptive Type-II progressively hybrid censoring with binomial removals, *J. Stat. Comput. Sim.*, **93** (2023), 1077–1103. https://doi.org/10.1080/00949655.2022.2127149
21. H. K. Yuen, S. K. Tse, Parameters estimation for Weibull distributed lifetimes under progressive censoring with random removeals, *J. Stat. Comput. Sim.*, **55** (1996), 57–71. https://doi.org/10.1080/00949659608811749
22. S. J. Wu, C. T. Chang, Inference in the Pareto distribution based on progressive type II censoring with random removals, *J. Appl. Stat.*, **30** (2003), 163–172. https://doi.org/10.1080/0266476022000023721
23. M. Sharafi, Inference of the two-parameter Lindley distribution based on progressive type II censored data with random removals, *Commun. Stat.-Simul. Comput.*, **51** (2022), 1967–1981. https://doi.org/10.1080/03610918.2019.1691226

24. E. M. Almetwally, Statistical inference for a one-parameter lifetime model under unified progressive hybrid censoring with binomial random removals, *AIMS MATH.*, **11** (2026), 211–242. https://doi.org/10.3934/math.2026009

25. D. Kundu, Bayesian inference and life testing plan for the Weibull distribution in presence of progressive censoring, *Technometrics*, **50** (2008), 144–154. https://doi.org/10.1198/004017008000000217

26. A. Henningsen, O. Toomet, maxLik: A package for maximum likelihood estimation in R, *Computation. Stat.*, **26** (2011), 443–458. https://doi.org/10.1007/s00180-010-0217-1

27. M. Plummer, N. Best, K. Cowles, K. Vines, CODA: convergence diagnosis and output analysis for MCMC, *R News*, **6** (2006), 7–11.

28. M. Vahter, L. Friberg, B. Rahnster, Å. Nygren, P. Nolinder, Airborne arsenic and urinary excretion of metabolites of inorganic arsenic among smelter workers, *Int. Arch. Occ. Env. Hea.*, **57** (1986), 79–91. https://doi.org/10.1007/BF00381375

29. S. Kumagai, I. Matsunaga, Physiologically based pharmacokinetic model for acetone, *Occup. Environ. Med.*, **52** (1995), 344–352. https://doi.org/10.1136/oem.52.5.344

30. P. O. Peter, B. Oluyede, H. F. Bindele, N. Ndwapi, O. Mabikwa, The Gamma Odd Burr III-G Family of Distributions: Model, Properties and Applications, *Revista Colombiana de Estadística*, **44** (2021), 331–368. https://doi.org/10.15446/rce.v44n2.89320

31. S. K. Maurya, T. Goyal, A New Decreasing Failure Rate Distribution and Its Real Life Application, *Int. J. Stat. Reliab. Eng*, **10** (2023).

32. P. R. D. Marinho, R. B. Silva, M. Bourguignon, G. M. Cordeiro, S. Nadarajah, AdequacyModel: An R package for probability distributions and general purpose optimization, *PloS one*, **14** (2019), e0221487. https://doi.org/10.1371/journal.pone.0221487

33. R. Alotaibi, S. Dey, A. Elshahhat, Analysis of Progressively Type-II Inverted Generalized Gamma Censored Data and Its Engineering Application, *Computer Modeling in Engineering and Sciences (CMES)*, **141** (2024), 459–189. https://doi.org/10.32604/cmes.2024.053255

34. A. Elshahhat, H. M. Aljohani, A. Z. Afify, Bayesian and classical inference under Type-II censored samples of the extended inverse Gompertz distribution with engineering applications, *Entropy*, **23** (2021), 1578. https://doi.org/10.3390/e23121578

35. F. R. De Gusmao, E. M. Ortega, G. M. Cordeiro, The generalized inverse Weibull distribution, *Stat. Pap.*, **52** (2011), 591–619. https://doi.org/10.1007/s00362-009-0271-3

36. E. Chiodo, P. D. Falco, L. P. D. Noia, F. Mottola, Inverse Log-logistic distribution for Extreme Wind Speed modeling: Genesis, identification and Bayes estimation, *AIMS Energy*, **6** (2018), 926–948. https://doi.org/10.3934/energy.2018.6.926

37. S. Lee, Y. Noh, Y. Chung, Inverted exponentiated Weibull distribution with applications to lifetime data, *Commun. Stat. Appl. Meth.*, **24** (2017), 227–240. https://doi.org/10.5351/CSAM.2017.24.3.227

38. A. A. Osi, S. A. Sabo, I. Z. Musa, Inverted dagum distribution: Properties and application to lifetime dataset, *Reliability: Theory and Applications*, **19** (2024), 595–604.

39. A. M. Basheer, Alpha power inverse Weibull distribution with reliability application, *J. Taibah Univ. Sci.*, **13** (2019), 423–432. https://doi.org/10.1080/16583655.2019.1588488

40. A. M. Abouammoh, A. M. Alshingiti, Reliability estimation of generalized inverted exponential distribution, *J. Stat. Comput. Sim.*, **79** (2009), 1301–1315. https://doi.org/10.1080/00949650802261095
41. K. Fatima, S. P. Ahmad, The Exponentiated Inverted Exponential Distribution, *Journal of Applied Information Science*, **5** (2017), 35–41. https://doi.org/10.18576/sjm/050106
42. A. M. Abd AL-Fattah, A. A. El-Helbawy, G. R. Al-Dayian, Inverted Kumaraswamy distribution: Properties and Estimation, *Pak. J. Stat.*, **33** (2017), 37–61.
43. C. Kleiber, S. Kotz, *Statistical Size Distributions in Economics and Actuarial Sciences*, 2003, Wiley and Sons, Inc, Hoboken, NJ, USA. https://doi.org/10.1002/0471457175
44. M. S. Khan, G. R. Pasha, A. H. Pasha, Theoretical analysis of inverse Weibull distribution, *WSEAS Transactions on Mathematics*, **7** (2008), 30–38.